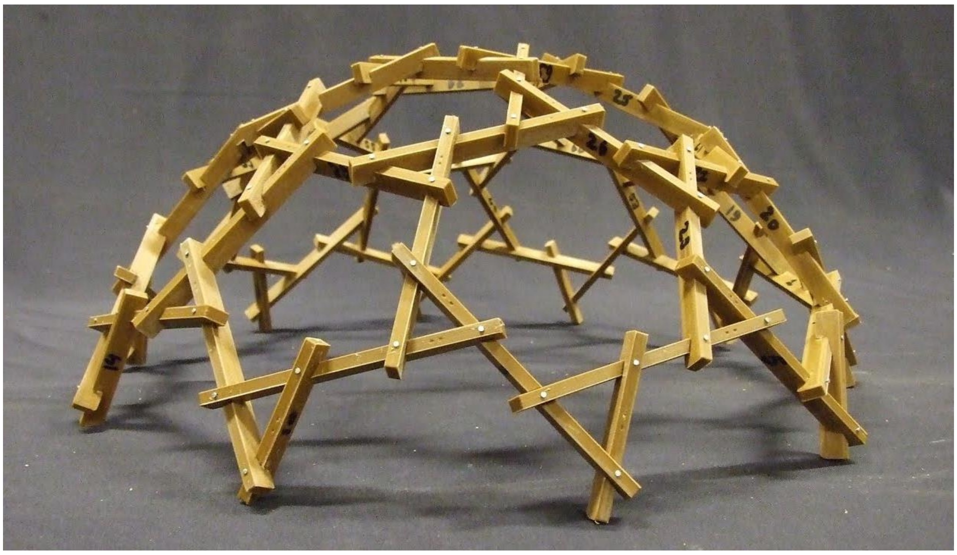

A STRUCTURAL ANALYSIS OF TIMBER RECIPROCAL FRAMES

Examining the influence of the connections, linking pattern and engagement length on the structural behavior of reciprocal frames

BACHELOR THESIS
CIVIL ENGINEERING
TU DELFT
Wouter Schrama
4728211
14-06-2021

TU Delft

A structural analysis of timber reciprocal frames

Examining the influence of the connections, linking pattern and engagement length on the structural behavior of reciprocal frames

By

Wouter Schrama

in partial fulfilment of the requirements for the degree of

Bachelor of Civil Engineering
Faculty of Civil Engineering and Geosciences
at the Delft University of Technology

Student number:	4728211
Date:	June 14, 2021
Supervisors:	Dr. ir. H.R. Roel Schipper
	Dr. ir. P.C.J. Pierre Hoogenboom

TU Delft

Preface

In front of you lies a bachelor thesis about the structural behavior of timber reciprocal frames. This thesis is written in order to complete the Bachelor of Civil Engineering at Delft University of Technology in the academic year of 2020 – 2021.

In earlier theses about timber reciprocal frames, certain structures were designed with the use of reciprocal frames. A design for a structure consisting of reciprocal frame was carried out, without explanations about why that particular design was chosen. This gap in the theses made me curious on the structural behavior of timber reciprocal frames and what influence certain parameters have on this. The thesis goes from identifying these parameters to determining their influence on the structural behavior.

I would like to thank Dr.ir. H.R. Schipper and Dr.ir. P.C.J. Hoogenboom for their help and guidance during the process of writing my bachelor thesis. Not only did they give advice about the content of the thesis, but also did they help me whenever I got stuck and was not able to carry on writing my thesis.

Wouter Schrama
Delft, the Netherlands
June 14, 2021

Abstract

New construction methods are invented to counteract the climate change. One of these is circular construction, in which building materials are being reused. Using waste wood to build new structures is such a method. A specific manner of building with this wood is to design a structure consisting of reciprocal frames. This method makes efficient use of shorter beams to bridge larger spams. However, reciprocal frames come in different configurations and consist of many parameters.

Therefore, the goal of this thesis is to determine the structural behavior of reciprocal frames and the influence of parameters on its behavior. This is done by conducting a literature study to determine what a reciprocal frame defines and what its parameters are. Thereafter, models are made in Rhino-GH with the use of Karamba3D, which is a parametric structural engineering tool, to examine the structural behavior.

A single reciprocal frame is a three-dimensional grid structure constructed of a closed circuit of mutually supporting beams. This means a structure of at least three beams, in which the beams are supported by each other.

The parameters of this structure that are analyzed are:

1. The type of connection between beams
2. The linking pattern of multiple RF-units
3. The engagement length

Different types of connections constrain the beams in different directions. Using connections that left the beams unconstrained in rotational direction left the RF-unit only loaded in bending and shear. Applying more rigid connections, which constrained the beams in both translational as rotational directions, introduced torsional moments in the beam but showed a decrease in shear.

Multiple RF-units can be linked in two ways, mirrored one-way or two-way. In the first geometry, the supportive beams in a RF-structure are loaded by two beams positioned in the same direction. The second option has the supported beams positioned in opposite directions. Results showed that for larger engagement lengths the two-way mirrored geometry has a stimulating effect on the torsional moments but is loaded less in bending and in shear than the one-way mirrored geometry.

The engagement length is the distance between the supported beam and the supportive beam. The bending moment showed in increase as the engagement length increased. The opposite holds for the shear force, which decreased for larger engagement lengths. The torsional moments were highest for relatively small and large engagement lengths.

Furthermore, only for the smallest engagement length did the shear force become normative in the failing of the structure. For all other engagement lengths, the bending moment was critical.

Contents

1. Introduction

Among the space structures is a method called reciprocal frames. Its characteristics allow for many various shapes and configurations. This thesis zooms in on these possibilities to examine the structural behavior of these reciprocal frames and its parameters.

1.1. Research question and goal

Climate change is a growing concern in the building industry. At global level, 24% of the materials extracted from the lithosphere is used for the building construction section (Bribián et al., 2011). Furthermore, the extraction, processing, and transportation of these raw materials in the building industry provide for high pollutions (Morel et al., 2001), with the building sector responsible for approximately one-third of the global carbon emissions (Nußholz et al., 2019). The depletion of these materials also results in higher building costs (Recycling Netwerk Benelux, 2011).

Because of this, durable construction is more important than ever. Research is being conducted to invent new building techniques that reduce the environmental impact. One of these techniques is circular building, where materials are being utilized that are otherwise waste. An example of circular building is reusing waste wood. One way to reuse wood is to build new structures with this waste wood. For this latter option, a specific method of building is possible, namely using timber reciprocal frames. This way, a structure that covers a large span can be designed reusing shorter beams.

This method brings many possibilities, as well as complexities. A structure made out of reciprocal frames often has a complex shape consisting of many beams and joints. Different ways of linking the frames result in different patterns and configurations of the frames. All these parameters make the reciprocal frames a complex building technique. When designing a structure consisting of reciprocal frames choices have to be made about these parameters.

Therefore, this thesis aims to get an insight in the structural behavior and failure modes of different reciprocal frames. The influence of different parameters and elements of reciprocal frames on their structural behavior is analyzed. Finally, the report is meant to serve as a help when designing a structure with the use of reciprocal frames. The report could be used as background information or as a guideline upon which the first design can be made.

The research question that will be answered is:

What is the structural behavior of
different forms of timber reciprocal frames?

Since this question cannot be answered directly, further information has to be sought. This thesis will therefore first examine what a reciprocal frame defines and what kind of different reciprocal frames exist, explaining the various parameters of reciprocal frames. Thereafter, the behavior of these frames will be examined as well as the impact of their parameters. Finally, the loading in which these structures tend to fail are addressed.

1.2. Methodology

In order to gain knowledge about reciprocal frames, a literature study is conducted. This helps understand the reciprocal frames and identify their parameters. With this knowledge, the parameters that have an influence on the geometry and structural behavior of reciprocal frames are determined. These are then modelled in Rhino-GH, which is a plug-in for Rhino in which a parametric model can be created writing a script. Using Karamba3D, this model can then be structurally analyzed. Karamba3D is a parametric structural engineering tool, which uses finite element method to analyze the response of three-dimensional constructions. It can combine the parametric geometry models created in Rhino-GH with finite element calculations. Parameters can easily be adjusted after which Karamba3D instantly recalculates the model. The results following from these models are then analyzed after which their influence on the structural behavior of reciprocal frames can be determined.

1.3. Reading guide

In the next chapter, the results of the literature study are given. The definition of a reciprocal frame and its parameters are determined, after which the analyzed parameters are identified. The first parameter, the connection between the beams, is then examined in the third chapter. Thereafter, in chapter 4, the influence of the linking method is analyzed. In chapter 5, two spans are modelled in which these parameters are combined. The third parameter, the engagement length, is then included and parametrically modelled so that its influence can be examined. The conclusion and recommendations then follow in chapter 6.

2. Reciprocal frames

This chapter explores the reciprocal frame and its parameters. The chosen parameters for analysis are identified.

2.1. What is a reciprocal frame

A reciprocal frame is a three-dimensional grid structure constructed of a closed circuit of mutually supporting beams (Chilton et al., 1995). This means a structure of at least three beams, where one outer end rests on a support and the other end is supported by the following beam. This procedure is followed until a closed loop is formed. Complicated grids can be constructed when using multiple reciprocal frame units. As a result of its self-supporting characteristic, no supports are needed midway the construction but only at the perimeter. Furthermore, these units can be dissembled and re-assembled at a different location, which makes them highly cost-efficient (Song et al., 2013).

2.2. Aspects of reciprocal frames

When defining a reciprocal frame, Larsen implies that the following parameters (see fig. 1) are of importance (2008):

- The number of beams (n)
- Radius through outer supports (r_o)
- Radius through inner supports (r_i)
- Total height of the reciprocal frame (H)
- Vertical eccentricity of beams (h_2)
- Length of the beams (L)

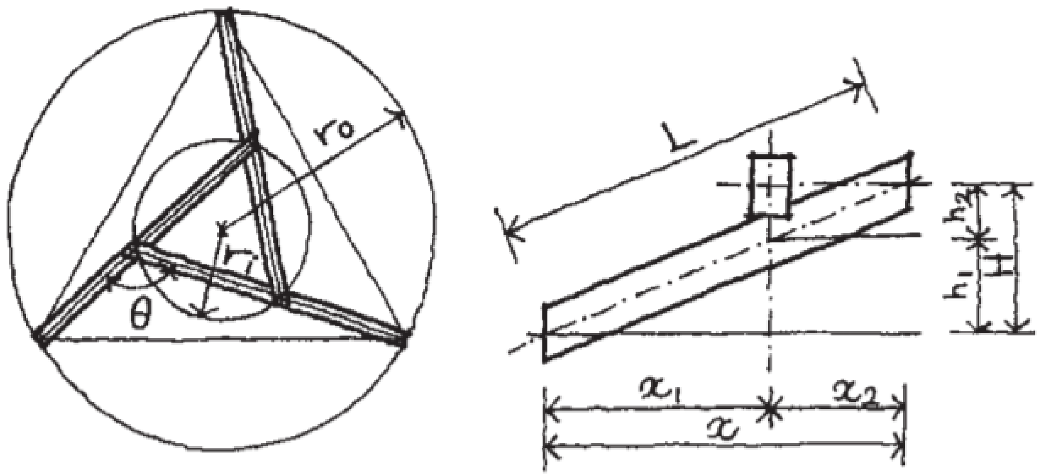

Figure 1: Parameters of a reciprocal frame (Larsen, 2008)

Changing these parameters not only determines the geometry of the frame but also the structural behavior. Changing the number of beams changes the shape of a single RF-unit, which on its turn could determine the grid pattern. Adjusting the eccentricity defines the composition of the grid. If the eccentricity is equal to zero, a planar grid is designed, whereas an eccentricity of larger than zero will result in a three-dimensional composition.

Another aspect of the reciprocal frames is its connections. The most-used type of connection is the notched connection. This way, the beams are pre-cut and afterwards locked in these notches, as shown in figure 2. A big disadvantage of this method is that it reduces the bending moment and shear capacity of the beam, due to the loss of cross-sectional area (Rizutto & Larsen, 2010).

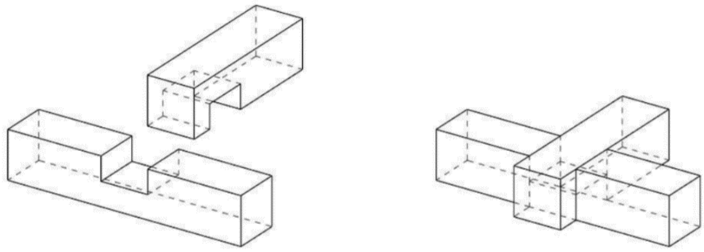

Figure 2: Notched connection (Gustafsson, 2016)

Another way is to rely on the friction between both beams. This method is also called superposition and can be seen in figure 3. The beams are placed on top of each other, transferring vertical loads to the underlying beam and resisting horizontal loading by friction. An advantage is that the cross-sectional area is not affected (Larsen, 2008).

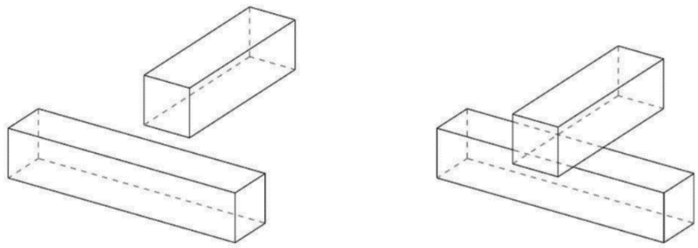

Figure 3: Superposition (Gustafsson, 2016)

A third type of connection is the dowel-type connection. This option would mean that the beams are connected by either dowels, nails, screws or bolts which are bored through both beams, which is shown in figure 4. These types of connections prevent translation, but the rotational constraints depend on different factors (Rizutto & Larsen, 2010).

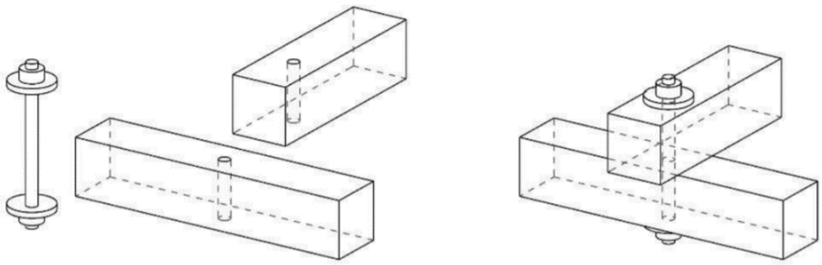

Figure 4: Dowel-type bolted connection (Gustafsson, 2016)

Lastly, an element could be used to secure a connection, which is called a coupler-type connection. Hereby the beams are clamped together to raise the mutual friction. This can be done with either ropelike or steel elements. An example of a steel clamped connection is shown in figure 5.

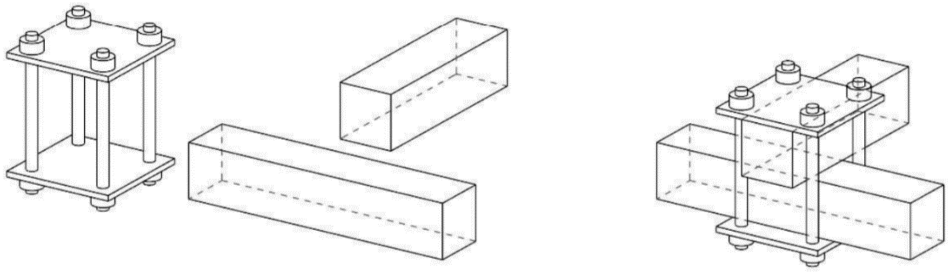

Figure 5: Coupler-type clamped connection (Gustafsson, 2016)

The mentioned aspects concern a single reciprocal frame, but a structure consisting of multiple reciprocal frames has characteristics of its own. Logically, the number of beams per reciprocal frame determine the shape of a single RF-unit, but this does not immediately define the pattern of the RF-structure. The way the frames are linked plays a role in the geometry of the structure as well, as is shown in figure 6. In both structures, a RF-unit with four beams is used. However, these are connected in different ways. In the left picture, the frames are mirrored in one direction only (vertically or horizontally). As a result, the supportive beam is loaded by two beams positioned in the same direction. In the right picture, the connected frames are mirrored in two directions, vertically as well as horizontally. The supportive beam is now loaded by two beams both positioned in opposite directions.

This has an influence on how the force exerted by a beam is distributed. Note that the beams are supported at their ends by other beams. In the midsection they give support to other beams. Therefore, the force is repeatedly distributed to the endpoints of the beam. This distribution is shown in figure 6. The red dot represents the force a beam exerts on its supportive beam. Its distribution is then shown in three steps, in which the first step is given in red, the second in blue and the last step in green.

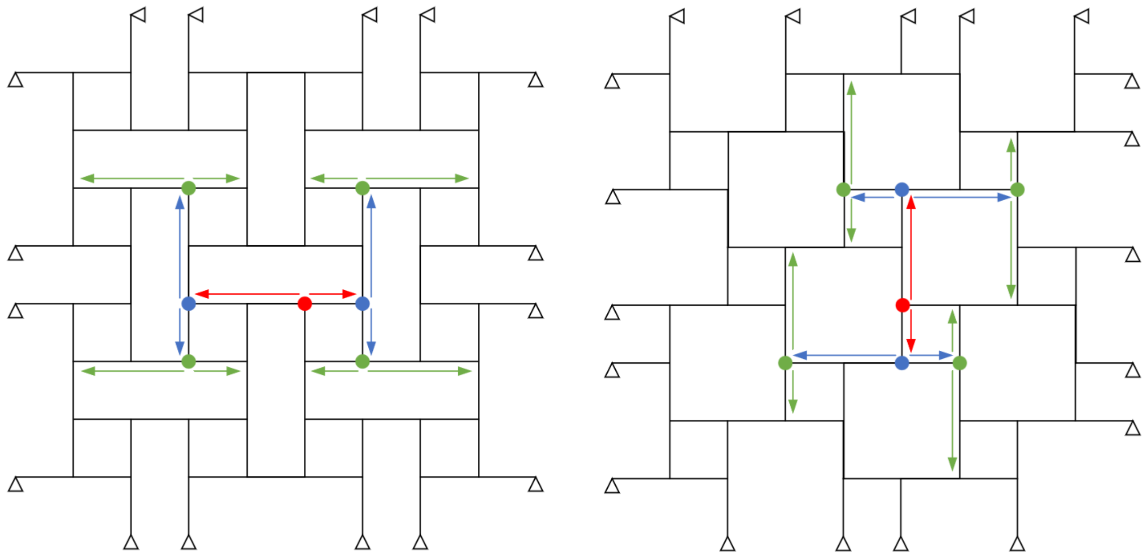

Figure 6: Force distribution for a one-way mirrored span (left) and a two-way mirrored span (right)

2.3. Materials

Reciprocal frames are not necessarily limited to a few materials, but the use of certain materials has its advantages. Since it is a self-supporting construction, a low self-weight is desired. Also, due to the growing concern of the climate change, durable resources are preferably used. As explained in chapter 1, one of the possibilities is reusing materials. Therefore, (waste)wood is a good building material to create reciprocal frames (Larsen, 2008). This thesis will focus on reciprocal frames made out of C24 timber. The strength and stiffness properties can be found in figure 7.

	Class	C14	**C16**	**C18**	C20	C22	**C24**	C27	**C30**	C35	C40	C45	C50
Strength properties in N/mm²													
Bending	$f_{m,k}$	14	**16**	**18**	20	22	**24**	27	**30**	35	40	45	50
Tension parallel	$f_{t,0,k}$	7,2	**8,5**	**10**	11,5	13	**14,5**	16,5	**19**	22,5	26	30	33,5
Tension perpendicular	$f_{t,90,k}$	0,4	**0,4**	**0,4**	0,4	0,4	**0,4**	0,4	**0,4**	0,4	0,4	0,4	0,4
Compression parallel	$f_{c,0,k}$	16	**17**	**18**	19	20	**21**	22	**24**	25	27	29	30
Compression perpendicular	$f_{c,90,k}$	2,0	**2,2**	**2,2**	2,3	2,4	**2,5**	2,5	**2,7**	2,7	2,8	2,9	3,0
Shear	$f_{v,k}$	3,0	**3,2**	**3,4**	3,6	3,8	**4,0**	4,0	**4,0**	4,0	4,0	4,0	4,0
Stiffness properties in kN/mm²													
Mean modulus of elasticity parallel bending	$E_{m,0,mean}$	7,0	**8,0**	**9,0**	9,5	10,0	**11,0**	11,5	**12,0**	13,0	14,0	15,0	16,0
5 percentile modulus of elasticity parallel bending	$E_{m,0,k}$	4,7	**5,4**	**6,0**	6,4	6,7	**7,4**	7,7	**8,0**	8,7	9,4	10,1	10,7
Mean modulus of elasticity perpendicular	$E_{m,90,mean}$	0,23	**0,27**	**0,30**	0,32	0,33	**0,37**	0,38	**0,40**	0,43	0,47	0,50	0,53
Mean shear modulus	G_{mean}	0,44	**0,50**	**0,56**	0,59	0,63	**0,69**	0,72	**0,75**	0,81	0,88	0,94	1,00
Density in kg/m³													
5 percentile density	ρ_k	290	**310**	**320**	330	340	**350**	360	**380**	390	400	410	430
Mean density	ρ_{mean}	350	**370**	**380**	400	410	**420**	430	**460**	470	480	490	520

Figure 7: Strength classes for softwood (CEN, 2016)

2.4. Chosen parameters

It can be concluded that a reciprocal frame is defined by many different parameters. Using more beams per RF-unit results in different shapes and applying a vertical eccentricity results in a curved structure. However, some parameters play a role in every configuration. In every RF-structure, a decision on how to connect the beams is made. Furthermore, despite the shape of the RF-units, a choice has to be about how to link the different RF-units and the engagement length. This comes back for RF-structures consisting of triangular, rectangular, or other RF-units, but also when combining different RF-units.

As a result of the literature study, the chosen parameters for analysis are:

1. Type of connections between the beams
2. Linking pattern of multiple RF-units
3. The engagement length

However, it is important to bear in mind that these are not the only parameters that influence the structural behavior. Further research could be done to examine the influence of other parameters.

3. Connection between the beams

This chapter includes an analysis of the influence of the connections on the structural behavior of a single reciprocal frame. First, this is done via an analytical approach, where calculations by hand will be done. After that, a model is created using Karamba3D, which is checked with the analytical results in order to verify that the model is representative for the behavior of a real reciprocal frame.

3.1. Schematizing the connections

The connections between the beams play a major role in the structural behavior of the reciprocal frame. As explained in section 2.2., different methods of connecting the beams are possible. Normally, the connections would have a certain translational and rotational stiffness. However, determining the stiffness of different types of connections goes beyond the scope of this thesis. The influence of different connections on the structural behavior is analyzed and therefore, as a simplification, the connections are assumed to be either hinged or fully fixed.

As of the connection, using superposition as a way to connect the beams would mean the beam end is not constrained in rotational direction. The rotational stiffness is then zero and so it will be schematized as a hinged connection. In case the beams are connected via notches, the beam will be fixed in more directions than just vertically. Therefore, there will be rotational constraints and thus rotational stiffness. These connections are simplified as fixed connections.

3.2. The reciprocal frame

A simple reciprocal frame consists of four beams, where every beam is supported on one end by a pinned perimeter support (A1, A2, A3 and A4) and on the other by another beam (B1, B2, B3 and B4). The connection between the beams acts as a support. The type of support depends on the kind of connection that is used. Somewhere along the beam it is giving support to another beam. The distance between the supported beam and the supportive beam is called the *engagement length.* From now on, the beam acting as a support is called the *adjacent* beam, whereas the beam exerting load is called the *preceding* beam. The reciprocal frame used for analysis is shown below in figures 8 and 9, in which the engagement length is shown as x.

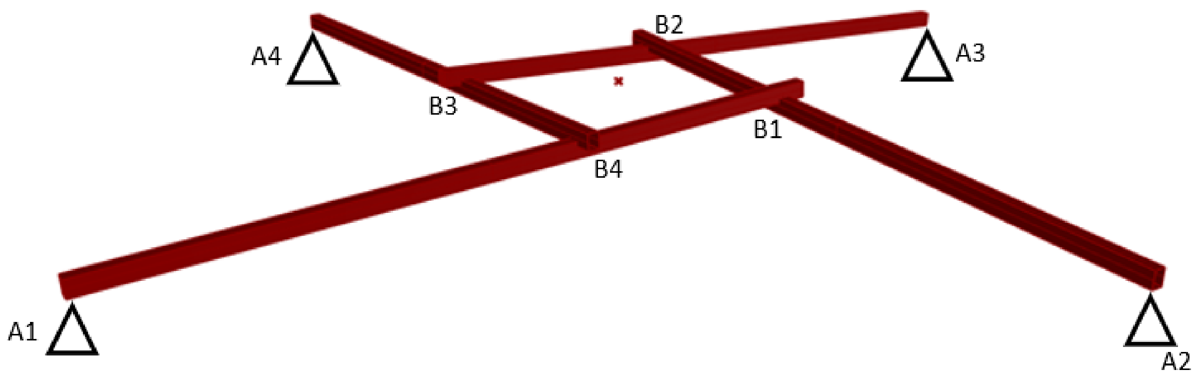

Figure 8: Reciprocal frame created in Rhino-GH

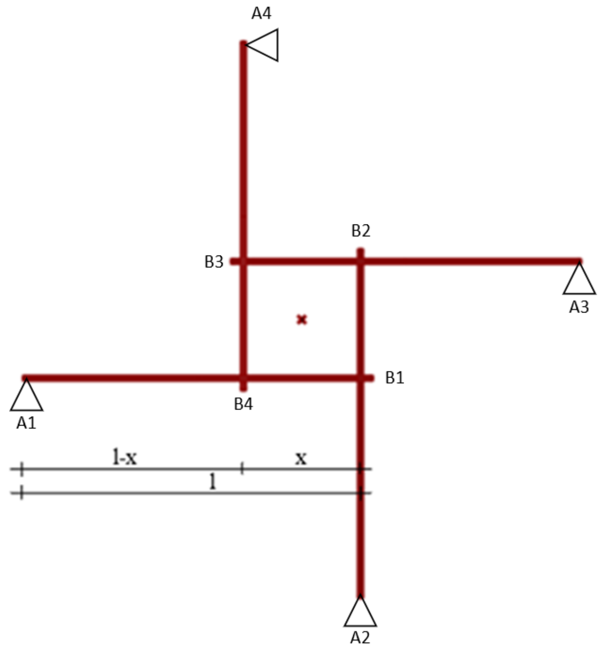

Figure 9: Reciprocal frame created in Rhino-GH

3.3. Analytical approach

First, a reciprocal frame using superposition is analyzed and thereafter one with notched connections. The frames are assumed to be loaded with a uniformly distributed load, for example self-weight. A point load F is added at a distance x from the beam end, which is exerted by the preceding beam. To clarify some of the following calculations, the local axes of a beam are defined in figure 10.

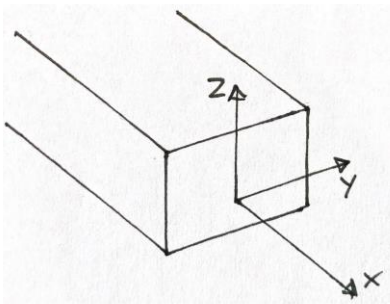

Figure 10: Local axis of a beam

3.3.1. Hinged connections

In case the connections between the beam are hinged, both ends of the beam are supported by a pinned support. A single beam of the RF-unit can then be schematized as a simply supported beam. The result is shown in in figure 11.

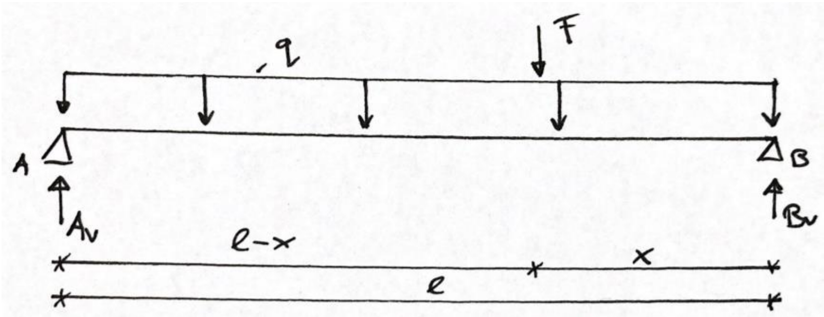

Figure 11: Schematization of Rf simply supported beam

Support reactions

First, the support reactions can be determined. Due to symmetry of the reciprocal frame, the vertical support reactions are the distributed load divided by the number of supports.

$$Av = q * l$$

Due to the hinged connection in B, this beam-end is supported by a pinned support. These supports cannot carry a bending moment, which means the bending moment in B is zero. With this condition, an expression for F can be determined.

$$\sum M|B = 0$$

$$Av * l - F * x - q * l * \frac{1}{2} * l = 0$$

$$F * x = Av * l - \frac{1}{2} * q * l^2$$

Substituting $Av = q * l$:

$$F * x = q * l^2 - \frac{1}{2} * q * l^2$$

$$F * x = \frac{1}{2} * q * l^2$$

$$F = \frac{q * l^2}{2 * x}$$

An expression for F has now been found. On a single beam, the sum of vertical forces must be zero. As a result of this vertical equilibrium, support reaction Bv can be determined.

$$\sum Fv = 0$$

$$Av + Bv - q * l - F = 0$$

Since $Av = q * l$, the expression becomes:

$$Bv = \frac{q * l^2}{2 * x} = F$$

This makes sense since the vertical support reaction in Bv becomes the point load F at the adjacent beam. Due to symmetry and total vertical equilibrium, Bv and F cannot be other than equal to each other, as is visualized in figure 12.

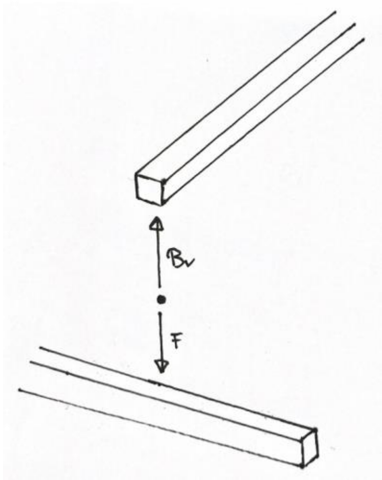

Figure 12: Sketch of node

The forces that form F are now explained. As explained before, F is the force that the preceding beam exerts onto the beam. Therefore, the reasons behind F are looked for in this preceding beam. A schematization is shown in figure 13, with the F being analyzed marked with a red circle. If done correctly, F should be similar to the F derived before with the sum of moments.

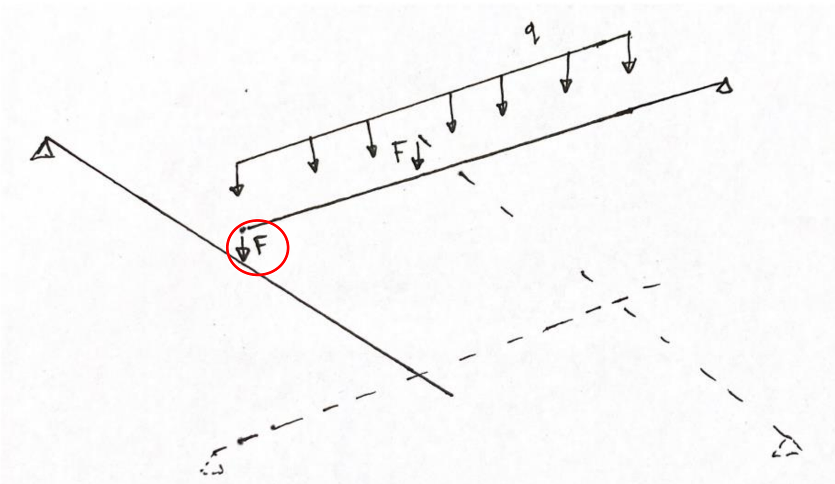

Figure 13: Schematization of loads on preceding beam

The uniform line load is divided equally over the two supports, which means $\frac{1}{2} * q * l$ is transferred to the adjacent beam and the other to the perimeter support. The distribution of F is dependent on its location along the beam. Again, taking the engagement length to be x, the part of F transferred to the preceding beam is:

$$\left(\frac{l-x}{l}\right) * F = \left(1 - \frac{x}{l}\right) * F$$

Therefore, the F analyzed is expressed via:

$$F = \frac{1}{2} * q * l + \left(1 - \frac{x}{l}\right) * F$$

$$F - \left(1 - \frac{x}{l}\right) * F = \frac{1}{2} * q * l$$

$$F * \left(1 - \left(1 - \frac{x}{l}\right)\right) = \frac{1}{2} * q * l$$

$$F * \frac{x}{l} = \frac{1}{2} * q * l$$

$$F = \frac{q * l^2}{2 * x}$$

As it should be, this F is similar to the F derived at the beginning of this section.

Section forces

With the support reactions and external forces known, the section forces and their distribution can be determined. The maximum moment in the beam is equal to:

$$M_{max} = Av * (l - x) - q * \frac{(l - x)^2}{2}$$

Substituting $Av = q * l$ and simplifying the equation, this becomes:

$$M_{max} = \frac{1}{2} * q * l^2 - \frac{1}{2} * q * x^2$$

The moment distribution diagram is shown in figure 14.

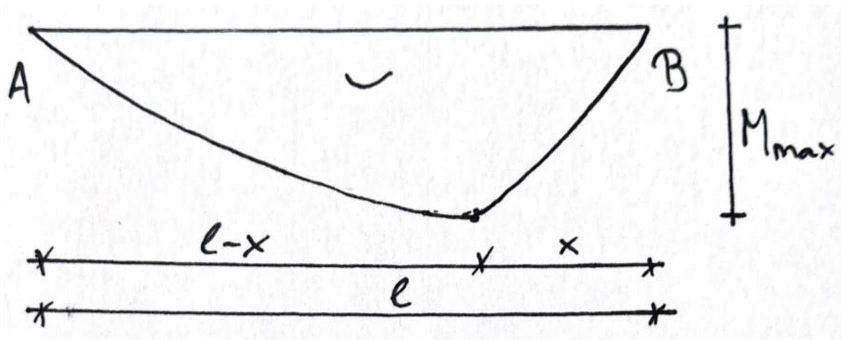

Figure 14: Moment distribution

The shear force diagram is shown in figure 15. At the intersection point, the shear force changes direction due to the point load F. Just at the left side of the intersection point, the shear force is equal to:

$$V_l = Av - q * (l - x)$$

Substituting $Av = q * l$:

$$V_l = q * l - q * (l - x)$$

$$V_l = q * x$$

At the right side, the shear force is equal to:

$$V_r = Bv - q * x$$

Substituting $Bv = \frac{q*l^2}{2*x}$ gives:

$$V_r = \frac{q * l^2}{2 * x} - q * x$$

$$V_r = q * \frac{(l^2 - 2 * x^2)}{2 * x}$$

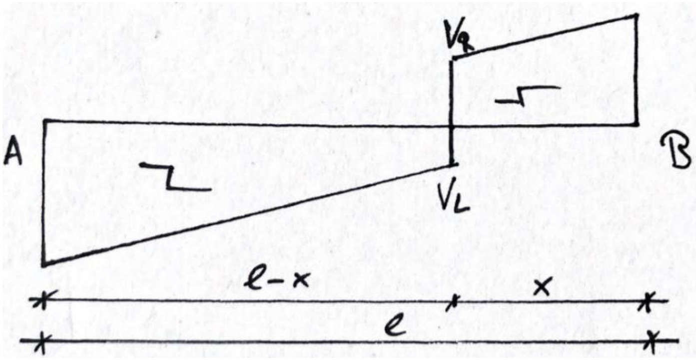

Figure 15: Shear force distribution

3.3.2. Fixed connections

The reciprocal frame behaves different when the connections between the beams are fixed. This way, the connection can take on bending moments. As explained in section 3.1., using notches would result in such a structure. Important to understand is the influence of the introduced bending moments on the section forces.

Due to the fixed connections, the reciprocal frame will have bending moments in all connections. First, the influence of the bending moment My around the y-axis is examined (see fig. 10 for definition for local axes). Note that this bending moment My results in a torsional moment Mx in the adjacent beam. The specific distribution of this torsional moment depends on the kind of perimeter support and connection. In this reciprocal frame with pinned supports, the torsional moment is transferred fully to the next connection. This torsional moment results in a bending moment My at every beam at the point of intersection with the preceding beam, as is schematized below in figure 16. Every connection includes both a My as a Mx and results in a Mx and a My in the adjacent beam.

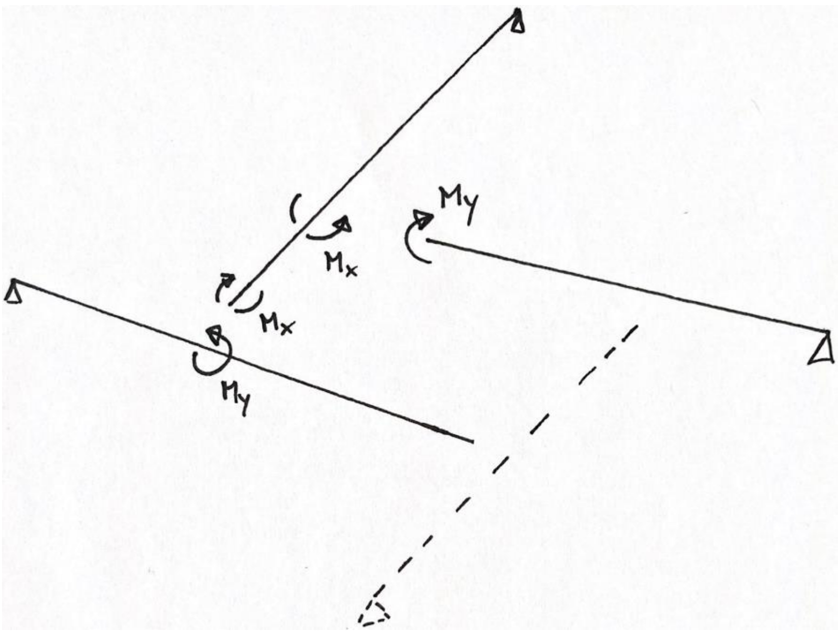

Figure 16: Distribution of torsional moment in RF-unit with fully fixed connections

As can be derived from figure 16 and because of symmetry, My at the intersection point is equal to My at the fixed connection, because it is a direct result of the My in the preceding connections.

Now that all the forces present on a single beam are known, the beam is schematized in figure 17.

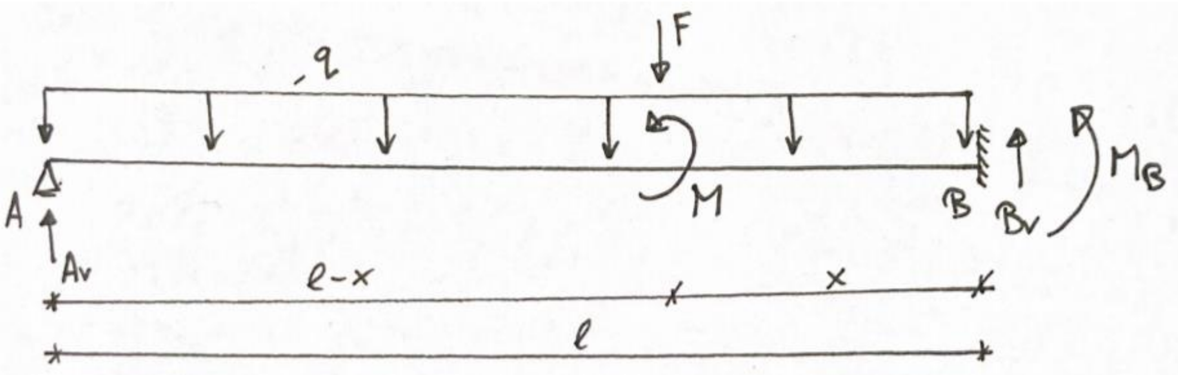

Figure 17: Schematization of RF-beam with fully fixed connection

Support reactions

Just like the reciprocal frame with hinged connections, the support reaction can be determined via symmetry and is the total load divided by the number of supports. This makes:

$$Av = q * l$$

From equilibrium of vertical forces, the support reaction in B can be determined.

$$Av + Bv - q * l - F = 0$$

$$Bv = F$$

As explained earlier, Mb is equal to M. Next, the sum of moments around B is taken.

$$\sum M|B = 0$$

$$Av * l - q * l * \frac{1}{2} * l - F * x - 2 * M_B = 0$$

Substituting $Av = q * l$ makes:

$$q * l^2 - \frac{1}{2} * q * l^2 - F * x - 2 * M_B = 0$$

$$2 * M_B = \frac{1}{2} * q * l^2 - F * x$$

$$M_B = \frac{1}{4} * q * l^2 - \frac{1}{2} * F * x$$

Section forces

As a result of the fixed connection and its introduced bending moment, the structure has become statically indeterminate. Using static equilibrium of forces does not suffice to determine the reaction and section forces. These are now also dependent of material and cross-sectional properties. The moduli and second moment of inertia have an influence on the behavior of the structure. Therefore, a model is made using Karamba3D in Rhino-GH, which is explained in section 3.4. Making use of this software, the shape of the bending moment, shear force and torsional moment distribution can be determined and shown in figure 18.

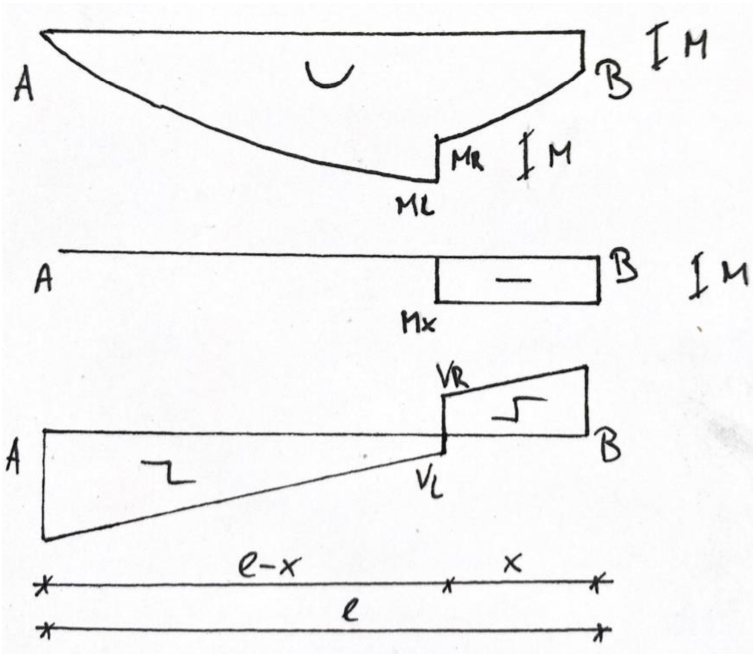

Figure 18: Bending moment (upper), torsional moment (middle) and shear force diagram (lower)

The equations for V_L and M_L are the same as the V_L and M_{max} for the reciprocal frame with hinged connections. Furthermore, the equations are:

$$M_B = M = M_x$$

$$M_R = M_L - M$$

$$V_R = V_L + F$$

3.4. Computational approach

To create this single RF-unit in Karamba3D, first the begin- and endpoint of every beam is created using the component *construct point*. A beam element is then created between all constructed points using *IndToBeam.* Having created the four beams for the RF-unit, the connections are modelled. To simulate a connection between the beams but keeping the eccentricity, a beam is created at every intersection point. Using the component *beam-joints*, these vertical beams are modelled as connections. This component adds a joint on either side of the beam, which can be independently adjusted. The lower joint is then left completely fixed to simulate a continuous beam, whereas the properties of the upper joint can be changed to simulate different types of connections. The length of this beam is then made very small (0.00001 m), as not to have an impact on the structural behavior of the RF-unit. The model can be seen in figure 19. Note that the length of the *beam-joints* is sized up in this figure to illustrate how the model works. When using the model, this length is made small again to remove the kink in the lower beam and make the model planar again.

The reason for using this method is to simulate the force distribution occurring in a reciprocal frame. Because of this small *beam-joint*, no forces are transferred to overlapping beams but only to the beam ends.

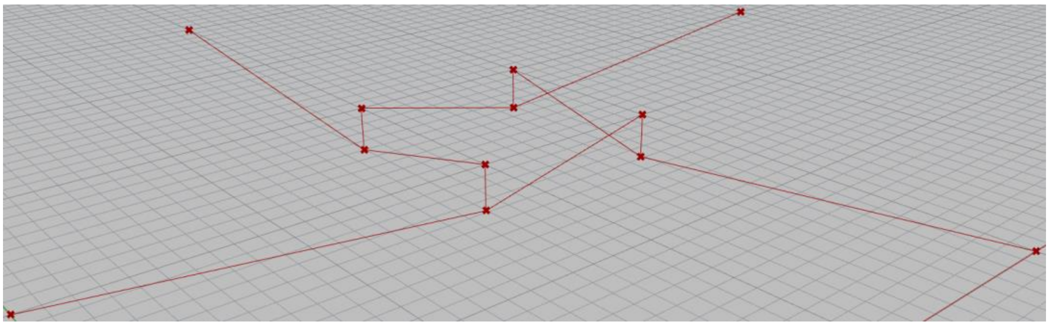

Figure 19: Rhino-GH model

In order to check if the model is correct, the outcome is checked with the results of section 3.3. The upper joint is given zero rotational constraints for the hinged connection and is changed to a fully fixed connection for the fixed connection.

A length of the beams l of 3 meters, engagement length x of 1 meter and a uniform line load q of 3 kN/m is used. Furthermore, the beams are given a rectangular cross-section of 0.2 x 0.1 m^2 (height x width), a Young's Modulus of 11000 MPa and a shear modulus of 690 MPa, which represents the C24 timber strength class (see figure 7 in section 2.3.).

3.4.1. Hinged connection

Using the equations derived in section 3.3. and the created Karamba3D model, the results of the analytical approach and the computational approach are compared and can be found in table 1. The outcomes from the Karamba3D model can be found in Appendix A.1.

Table 1: Results of analytical and computational approach for a RF-unit with hinged connections

	ANALYTICAL APPROACH	COMPUTATIONAL APPROACH
A_V	9 kN	8.99 kN
B_V (= F)	13.5 kN	13.49 kN
M_{MAX}	12 kNm	11.99 kNm
V_L	-3 kN	-2.99 kN
V_R	10.5 kN	10.49 kN

The results for this simple RF-unit are the almost exactly same for both approaches and therefore the Karamba3D model is assumed to be correct.

3.4.2. Fixed connection

Because of the statical indeterminacy the forces cannot be determined using the equilibrium of forces. The equation derived in section 3.3. for a reciprocal frame with fixed connections is:

$$M = \frac{1}{4} * q * l^2 - \frac{1}{2} * F * x$$

The moment M is still dependent on the force F, which remains unknown. However, the formula can still be used to check the model. If the model is correct, it will provide the right value for F. This value can then be used to calculate the other variables. Table 2 gives the results from both approaches. In Appendix A.2. the results from the Karamba3D model are presented.

Table 2: Results of analytical and computational approach for a RF-unit with fixed connections

	ANALYTICAL APPROACH	COMPUTATIONAL APPROACH
A_V	9 kN	9 kN
B_V (= F)	-	13.20 kN
M (= M_X, M_B)	0.15 kNm	0.15 kNm
M_L	12 kNm	12 kNm
M_R	11.85 kNm	11.85 kNm
V_L	-3 kN	-3 kN
V_R	10.20 kN	10.20 kN

Deriving F from the model and using it for the analytical approach gives the same outcomes and therefore also the model with fixed connections is also assumed to be correct.

3.5. Influence of connections

This section aimed to examine the influence of the connections on the structural behavior of a reciprocal frame.

Different type of connections means different constraints at the intersection point of the beams. Using superposition, in which only the vertical direction is constrained, would results in zero rotational stiffness. Therefore, the connections were modelled as hinged connections. This RF-unit is only loaded in shear and a bending moment along the beam. At the intersection point the bending moment equals zero. This is due to the fact that every preceding beam can rotate freely on top of the supportive beam and therefore it does not exert a bending moment.

The beams of a reciprocal frame can also be more rigidly connected. This way, the beam is also constrained in its rotational direction and as a result, it can exert bending moments on the supportive beam. Thus, fixed connections introduced a bending moment My and a torsional moment Mx in the beams. Together with this came a decrease of shear force in the connection. The value for V_R in table 2 is lower than for V_R in table 1.

4. Linking pattern of multiple RF-units

As explained in section 2.2. there are different ways to link RF-units as to form a grid, namely mirrored one-way and two-way. Extending a single RF-unit to a RF-structure consisting of multiple reciprocal frames introduces a new beam. This beam is not supported by perimeter supports anymore but is supported by two other beams. Also, it gives support to two beams instead of one. This introduced beam is shown in figure 20, with the two loads due to overlapping beams indicated with red dots. The left structure shows a beam loaded by two beams in the same direction, whereas the right structure shows a beam loaded by two beams in opposite direction.

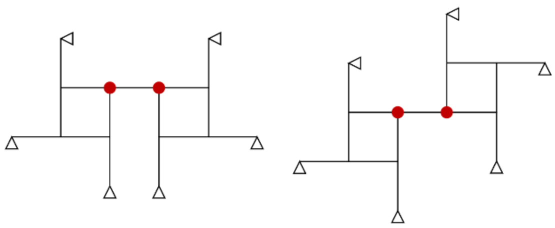

Figure 20: Double loaded beam

Linking four rectangular RF-units results in a closed circuit. Using the same method as explained in section 3.4., models are created in Rhino-GH. The difference in interaction of forces for both connections, as covered in chapter 3, are described.

4.1. Mirrored one-way

In case the linked RF-units are mirrored one-way, a beam is loaded by two beams that are positioned in the same direction. This results in a structure as shown in figure 21.

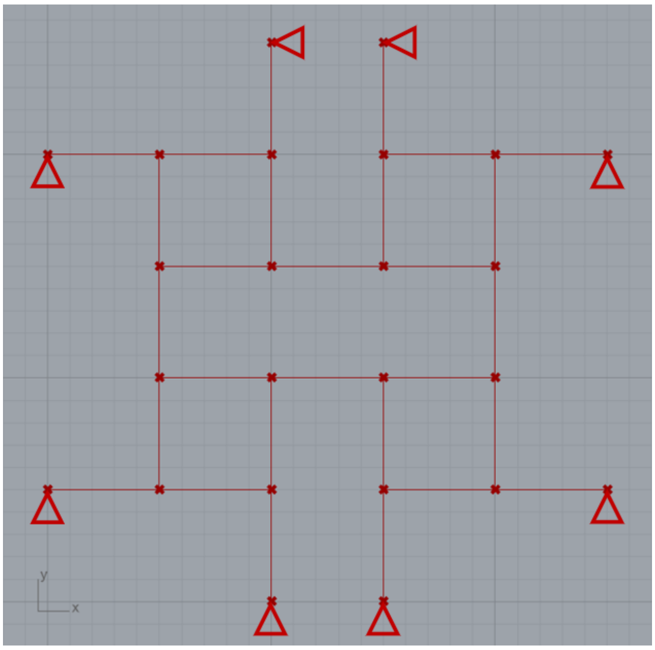

Figure 21: One-way mirrored RF-structure

4.1.1. Hinged connections

If the single beams are connected in a way as described in section 3.3.1., the double supported beam acts as a simply supported beam with two point loads and a uniformly distributed load. These point loads are both still vertically directed.

4.1.2. Fixed connections

As explained in section 3.3.2., extra bending moments are introduced if the connections between single beams are fixed. At the intersection points a bending moment My and a torsional moment Mx occur. Using a geometry where the linking of the RF-units is done in a one-way mirrored method, the bending moments My in the two preceding beams have the same direction. The torsional moments that result from these bending moments are therefore of the same direction as well and thus have a cancelling impact on each other. This occurrence is sketched in figure 22. Due to symmetry and as a result of this geometry, the middle sections of the beams are not loaded in torsion.

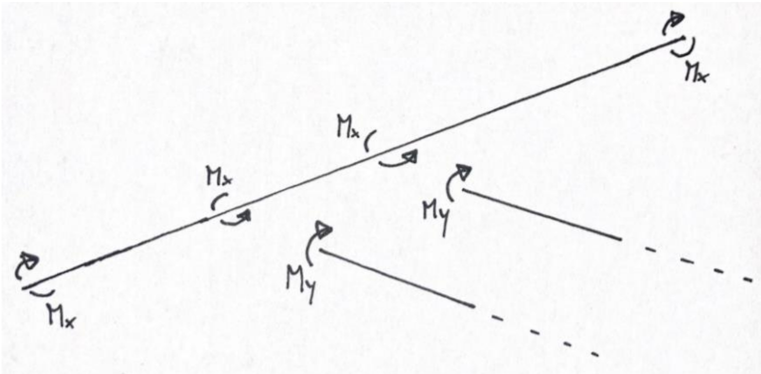

Figure 212: Torsional moments in one-way mirrored RF-structure

The corresponding torsional moment distribution is then as shown below in figure 23.

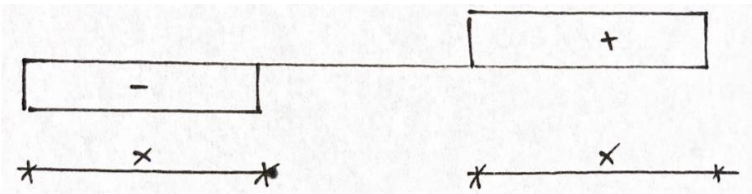

Figure 23: Distribution of torsional moment one-way mirrored RF structure

4.2. Mirrored two-way

As a consequence of linking RF-units in a two-way mirrored manner, the double loaded beam is loaded by two beams positioned in opposite directions. The structure then has the geometry as shown in figure 24.

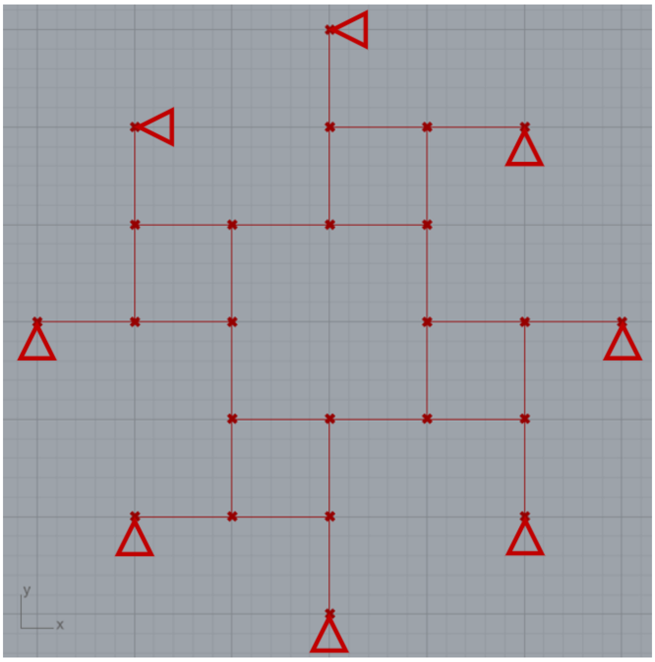

Figure 24: Two-way mirrored RF-structure

4.2.1. Hinged connections

The same explanation given in section 4.1.1. is valid for this structure with hinged connections at the intersection points of the beams. The hinged connections cannot take on a bending moment and thus cannot exert one. Again, the double loaded beams act as a simply supported beam loaded by two point loads and a uniformly distributed load.

4.2.2. Fixed connections

The consequence of this geometry is that the double loaded beam is loaded in opposite directions. Rigidly connecting single beams at their intersection points results in bending moments in the connections, but now these are opposite to each other. As a result, the two torsional moments that follow from these bending moments My have opposite directions as well. Therefore, they have a stimulating effect on one another resulting in larger torsional moments at the midsection of the double loaded beam. Figure 25 illustrates this interaction.

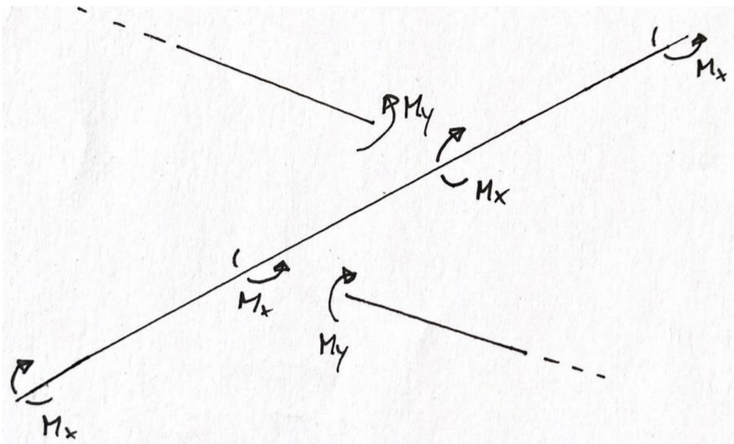

Figure 25: Torsional moments in two-way mirrored RF-structure

The shape of the torsional moment distribution belonging to this geometry is shown in figure 26.

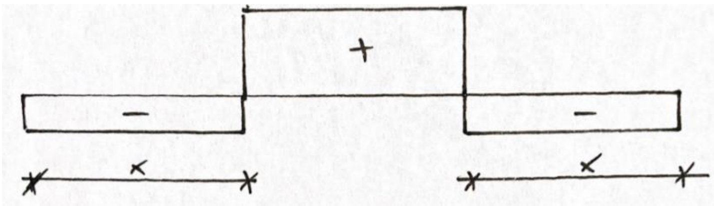

Figure 26: Distribution of torsional moment two-way mirrored RF-structure

4.3. Influence of linking pattern

This section zoomed in on the two different ways to link multiple RF-units and the influence it has on the structural behavior of reciprocal frames.

Linking the RF-units in a one-way mirrored method has a mitigating effect on the torsional moment. The bending moments exerted by supported beams are in the same direction, causing the torsional moments to be in the same direction as well. The midsection of the beam is therefore less loaded in torsional moment.

However, using a two-way mirrored method for linking RF-units has the contrary effect. The bending moments at the intersection points between single beams are now in opposite directions, whereupon the bending moments are of opposite directions as well. The torsional moments resulting from these bending moments are now opposite of each other, which leads to higher torsional moments at the midsection of the beam.

5. Engagement length

In this section, Karamba3D is used to model two spans consisting of reciprocal frames using both linking pattern. Using Rhino-GH, the engagement length can easily be adjusted as the Karamba3D analyses the structure. The maximum forces can then be used to identify the critical elements, by verifying the structure according to the Eurocode.

5.1. Dimensions and loads

Starting from the lower left side, a single RF-unit is modelled. From there, the linking pattern is repeated until a span of 9 x 9 m^2 is reached. At the perimeter, the span is supported by pinned supports.

The nodes are assumed to be fixed. First of all, because it is assumed that for most constructions where reciprocal frames are used, the beams are somehow rigidly connected at the intersection points, albeit via notching or using a dowel-type connection. Secondly, this makes the analysis more interesting as torsional moments are taken into account.

For this analysis, the beams again have widely used dimensions of 0.1 x 0.2 m^2 and are made of a C24 timber strength class. The Young's Modulus is therefore 11000 MPa and the shear modulus 690 MPa. An example of the spans with engagement lengths of 1 meter is shown in figure 27.

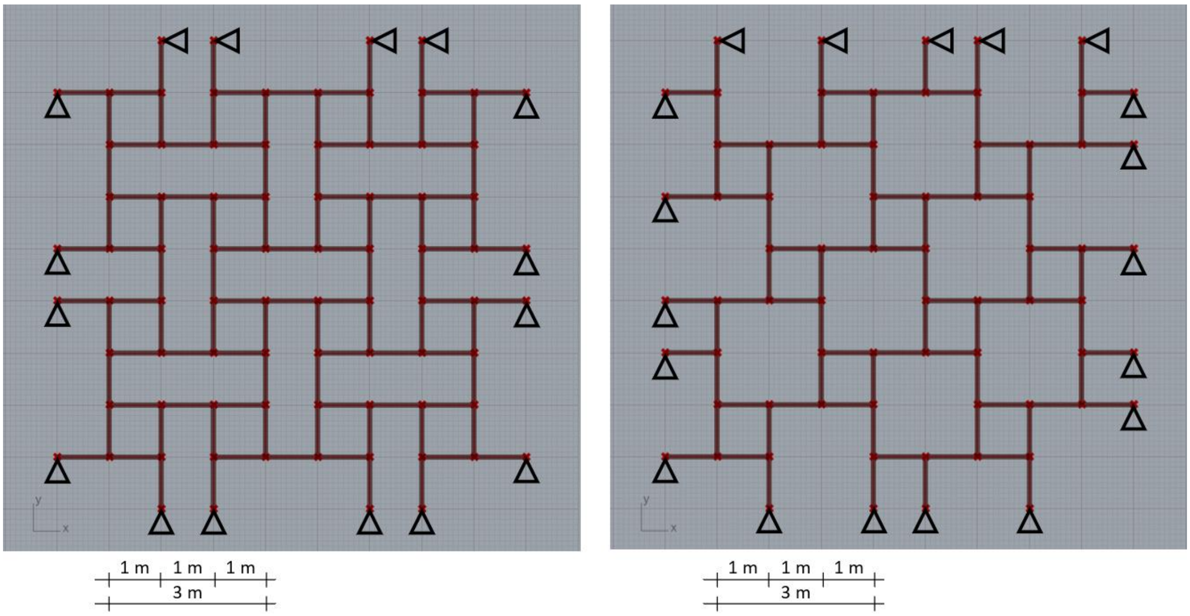

Figure 227: One-way mirrored RF-span (left) and two-way mirrored RF-span (right)

The loads are divided into self-weight and a variable load. The self-weight is dependent on the dimensions of the beam and is therefore:

$$width\ [m] * height\ [m] * \rho \left[\frac{kg}{m^3}\right] * 9.81 \left[\frac{m}{s^2}\right] = 0.1 * 0.2 * 420 * 9.81 = 0.0824\ kN/m$$

According to Eurocode 1, a standard variable load is $q_k = 0.4 \frac{kN}{m^2}$. For this thesis, this is assumed to be converted to $0.4\ kN/m$. As a result, the final uniformly distributed load on the structure is:

$$0.0824 + 0.4 = 0.4824\ kN/m$$

5.2. Verification formulas of Eurocode

The received loads will be verified according to the Eurocode. The relevant formulas are explained below.

5.2.1. Verification of bending strength

The structure has to resist the bending moments that occur. The stresses following the bending moment should not exceed the bending strength of the beam. In this case, the structure is loaded in bending in one direction only. Therefore, the formula to test bending strength is:

$$\frac{\sigma_{m,y,d}}{f_{m,y,d}} < 1$$

$$\sigma_{m,y,d} = \frac{M_{y,d}}{W_y}$$

$$f_{m,y,d} = k_{mod} * \frac{f_{m,k}}{\gamma_M}$$

Where:

$k_{mod} = 0.6$ for square cross-sections

$\gamma_M = 1.3$

$f_{m,k} = 24\ N/mm^2$

$W_y = 66.66 * 10^4\ mm^3$

$f_{m,y,d} = 11.1\ N/mm^2$

5.2.2. Verification of shear strength

Also, the shear stresses have to be resisted. The structure has to satisfy:

$$\tau_d < f_{v,d}$$

$$\tau_d = \frac{3 * V_d}{2 * b * h}$$

$$f_{v,d} = k_{mod} * \frac{f_{v,k}}{\gamma_M}$$

Where:

$f_{v,k} = 4\ N/mm^2$

$f_{v,d} = 1.85\ N/mm^2$

5.2.3. Verification of torsional strength

The last verification is the test on torsional shear strength. The structure may not exceed:

$$\tau_{tor,d} < k_{shape} * f_{v,d}$$

$$\tau_{tor,d} = \frac{M_t}{\alpha * b * h^2}$$

Where:

$k_{shape} = 1.3$ (see fig. 28, upper value is for circular profiles)

$\alpha = 0.246$ (see fig. 29, for this table b > t)

$$k_{\text{shape}} = \begin{cases} 1{,}2 \\ \min\begin{cases} 1+0{,}15\dfrac{h}{b} \\ 2{,}0 \end{cases} \end{cases}$$

Figure 238: Eurocode 5, values of k_{shape}

b/t	1.00	1.50	1.75	2.00	2.50	3.00	4	6	8	10	∞
α	0.208	0.231	0.239	0.246	0.258	0.267	0.282	0.299	0.307	0.313	0.333
β	0.141	0.196	0.214	0.229	0.249	0.263	0.281	0.299	0.307	0.313	0.333

Figure 249: Values for α

5.3. Results

Via Karamba3D the maximum forces occurring in the spans are obtained. For both spans the results are shown in the graphs below per engagement length. This makes a comparison between the two spans easier. The models with the bending moment, shear force and torsional moment distribution from Karamba3D can be found in Appendix B and C.

5.3.1. Maximum forces

Figure 30 shows the change in bending moments for different engagement lengths.

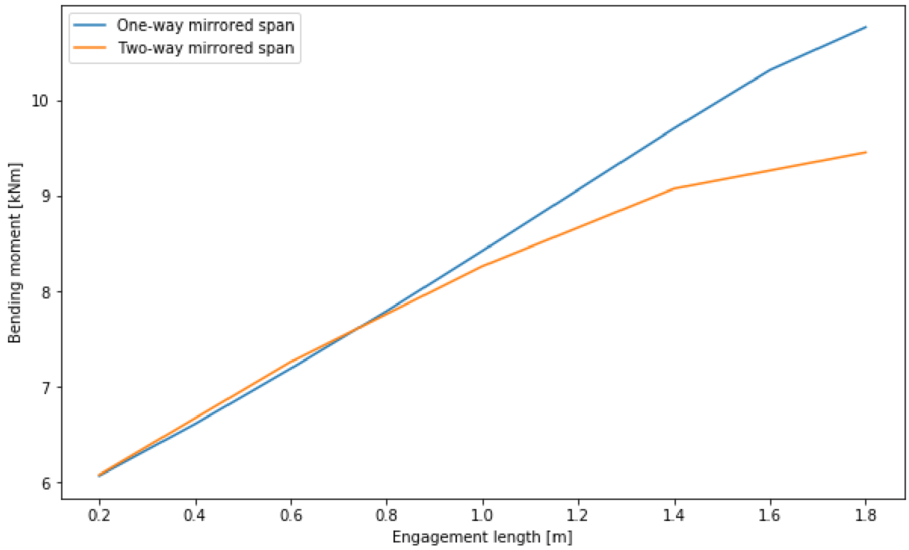

Figure 30: Maximum bending moment (kNm) vs engagement length

For both linking patterns, an increase in engagement length means in increase in bending moment. This makes sense, since larger engagement lengths mean larger RF-units. Therefore, the beams will get longer and as a result the occurring bending moments will increase.

Furthermore, the increase in bending moment shows a stagnating trend for the two-way mirrored span. An explanation for this is that the two-way mirrored span requires less material to bridge a larger span than the one-way mirrored span. In this case, less material means a lower total load and that results in lower bending moments. For larger engagement lengths, this becomes more relevant since the RF-units are larger.

In figure 31, the results for the shear force are shown.

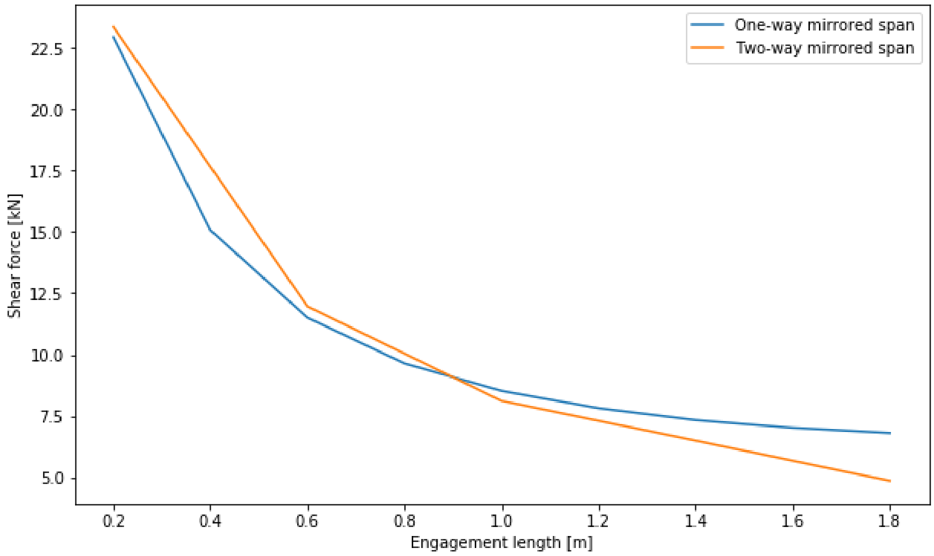

Figure 31: Maximum shear force (kN) per engagement length

Increasing the engagement length results in a decrease in the maximum shear force. An explanation for this is that for smaller engagement lengths, the point loads due to supported beams are located more closely to the connections. Therefore, a larger share of that point load will be transferred to this beam end then for larger engagement lengths. For larger engagement lengths, the forces are moved more closely together towards the midst of the beam. The distribution of the two forces following from the supported beams is then more equally divided and thus the maximum shear force decreases.

Just as for the bending moment, the two-way mirrored span has lower maximum shear force than the one-way mirrored span. The same explanation counts for this occurrence. For larger engagement lengths, the total load becomes relatively lower for two-way mirrored spans. This results in lower point loads exerted by the supported beams and hence ends in a lower maximum shear force.

Figure 32 presents the maximum torsional moment per engagement length.

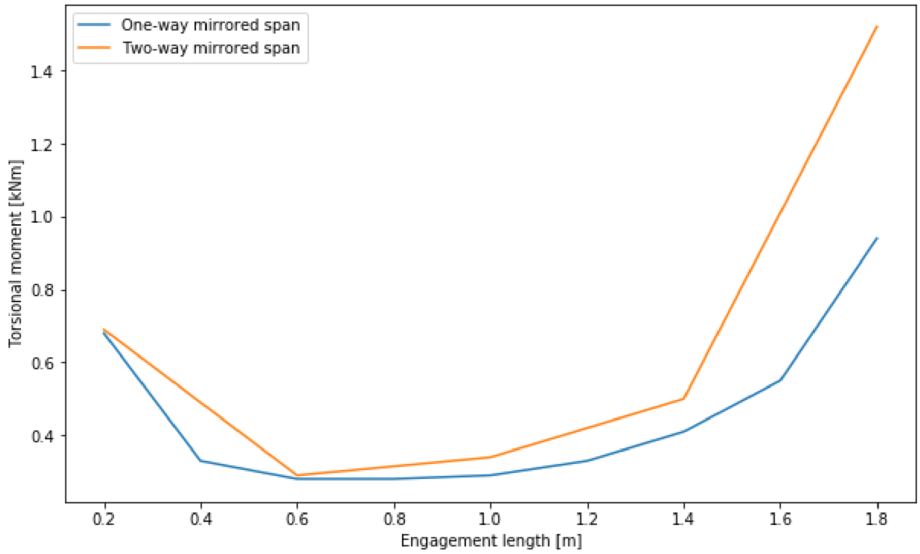

Figure 32: Maximum torsional moment (kNm) per engagement length

For relatively small and large engagement lengths, the torsional moment increases. Concerning small engagement lengths, the same theory counts as for the shear force. Small engagement lengths mean that a larger part of the bending moments occurring in the connections are transferred to the outer support (i.e., the supportive beam). However, for larger engagement lengths, the torsional moments following from My in the preceding beams are moved closely together. If these moments have opposite directions, this results in an increase in torsional moment in the midsection of the beam. As examined in chapter 4, this effect is most present in the two-way mirrored geometry. Note that this is remarkable, since the torsional moments are a direct result of the bending moment, and these are in fact smaller for the two-way mirrored span (see fig. 30).

5.3.2. Normative section force

In the graphs below the verification formulas are used in combination with the maximum forces. Figure 33 shows the results for the one-way mirrored span.

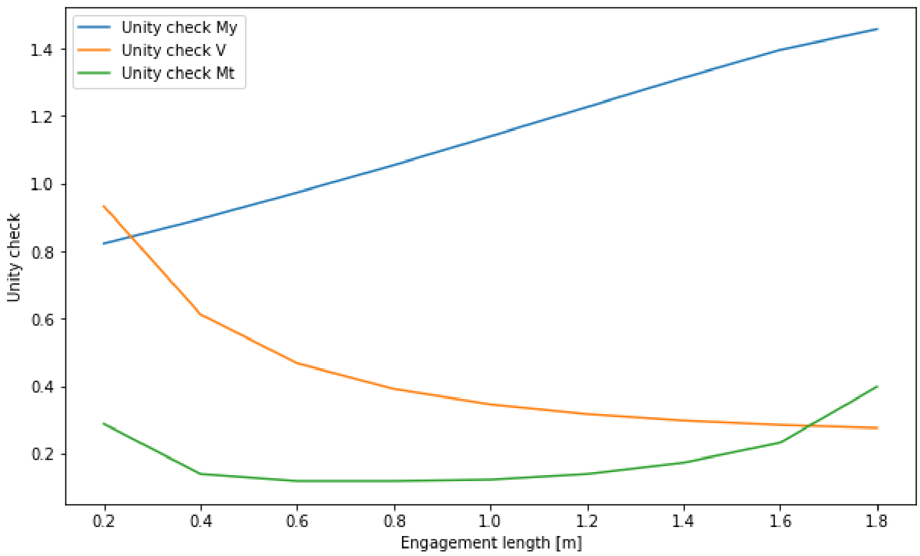

Figure 3325: Unity check vs engagement length for a one-way mirrored span

For the smallest applied engagement length, the shear force is most critical. However, for all other engagement lengths, the bending moment becomes the defining element in the failing of the RF-structure.

Figure 34 shows the results for the two-way mirrored span.

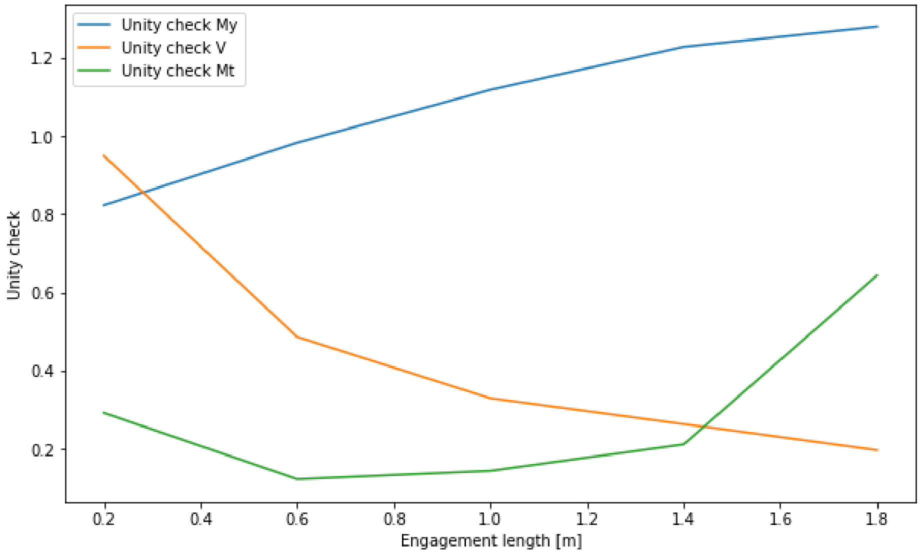

Figure 34: Unity check vs engagement length for a two-way mirrored span

Again, the bending moment is critical for all engagement lengths except for the smallest value. For the smallest value, the shear force is normative. The main difference is the increasing unity check for the torsional moment, which is a result of the torque-stimulating geometry of a two-way mirrored span.

6. Conclusion and recommendations

This thesis aimed to get an insight in the structural behavior of timber reciprocal frames. To achieve this, parameters are identified that play a role in the geometry of the reciprocal frames and their influence on the structural behavior is examined.

6.1. Conclusion

The analyzed parameters are:

1. The connections between the beams
2. The linking pattern of multiple RF-units
3. The engagement length

Different type of connections result in different constraint at the intersection point of the beams. In case the beams are not constrained in rotational directions, the beams are only loaded in bending moment and shear force. Using a more rigid connection causes the beams to be constrained in rotation. This introduces bending moments in the connections. As a result, the structure becomes loaded in torsion and showed in decrease in shear force.

The linking pattern plays a role in the geometry of structures consisting of reciprocal frames. Single RF-units can be linked in two ways, mirrored one-way or two-way. In a one-way mirrored geometry, the beams are loaded by two beams positioned in the same direction. This causes a mitigating effect on the torsional moments in the structure. Applying a two-way mirrored geometry has the beams loaded by two beams positioned in opposite directions. For larger engagement lengths, this stimulates the torsional moments occurring in the structure. However, the two-way mirrored span showed a lower maximum bending moment and shear force for larger engagement lengths.

The engagement length is the distance between the supported beam and the supportive beam.

- The bending moments showed an increase for larger engagement lengths. This can be explained due to the fact that for larger engagement lengths, the RF-units become larger. Longer beams result in larger bending moments.
- The shear forces showed the opposite trend. Increasing the engagement length meant a decrease in shear force. That is because for larger engagement lengths, the point loads due to the supported beams are moved to the center of the beam. As a result, the forces are distributed more equally over the beam.
- The torsional moments are the highest for very small and very large engagement lengths. For very small engagement lengths, a large part of the torsion created in the connection is transferred to the beam end. Using larger engagement lengths mean the torsional moments created in the connections are more equally distributed. However, these torsional moments can take on opposite directions. The combination of moving two opposite torsional moments more closely to each other results in higher torque at the midsection of the beams.

Finally, the normative load for the analyzed RF-structures is the bending moment. Only for the smallest engagement length did the shear force become the most critical.

6.2. Recommendations for future research

This thesis made use of some assumptions. The main assumption is to schematize the different type of connections as either hinged or fixed. This is done because the goal of the thesis is to determine the influence of different parameters on the structural behavior of reciprocal frames and not to obtain perfect numerical answers. However, in reality these connections have a certain translational and rotational stiffness. More detailed research could be conducted on the influence of the connections by including the actual stiffnesses.

Furthermore, similar analyses could be carried out for different geometries. For example, the research could be reconducted for structures consisting out of triangular reciprocal frames.

Lastly, different load cases could be included. For this thesis, a uniformly distributed line load was assumed. However, if a structure consisting out of reciprocal frames is designed as a supportive structure for a roofing or a flooring, tributary areas need to be included. Adjusting parameters then also has an influence on the distribution of the loads.

Bibliografie

Bribián, I. Z., Capilla, A. V., & Usón, A. A. (2011). *Life cycle assessment of building materials: Comparative analysis of energy and environmental impacts and evaluation of the eco-efficiency improvement potential.* Elsevier.

CEN. (2016). *EN-338:2016 Structural Timber - Strength classes.* CEN.

CEN. (2019). *Eurocode 1: Actions on structures.* CEN.

Chilton, J., Choo, B., & Popovic, O. (1995). *Reciprocal frames past, present and future.* University of Nottingham.

Gustafsson, J. (2016). *Connections in Timber Reciprocal Frames.* Gothenburg: Chalmers University of Technology.

Larsen, O. P. (2008). *Reciprocal Frame Architecture.* Elsevier.

Morel, J., Mesbah, A., Ogerro, M., & Walker, P. (2001). *Building houses with local materials: means to drastically reduce the environmental impact of construction.* Elsevier.

Nußholz, J. L., Rasmussen, F. N., & Milios, L. (2019). *Circular building materials: Carbon saving potential and the role of business model innovation and public policy.* Elsevier.

Recycling Netwerk Benelux. (2011). *Grondstoffenschaarste.* Opgehaald van Website van Recycling Netwerk Benelux: https://recyclingnetwerk.org/wp-content/uploads/2013/06/PDF-Notitie-Grondstoffenschaarste-Recycling-Netwerk.pdf

Rizutto, J., & Larsen, O. P. (2010). *Connection Systems in Reciprocal Frames and Mutually Supported Elements Space Structure Networks.* International Journal of Space Structures.

Song, P., Fu, C.-W., Goswami, P., Zheng, J., Mitra, N. J., & Cohen-Or, D. (2013). *Reciprocal Frames Structures Made Easy.* ACM Transactions on Graphics.

Soons, F., & van Raaij, B. (2014). *Quick Reference.* Delft University of Technology.

Appendix

A. Single RF-unit: section forces distribution

A.1. RF-unit with hinged connections

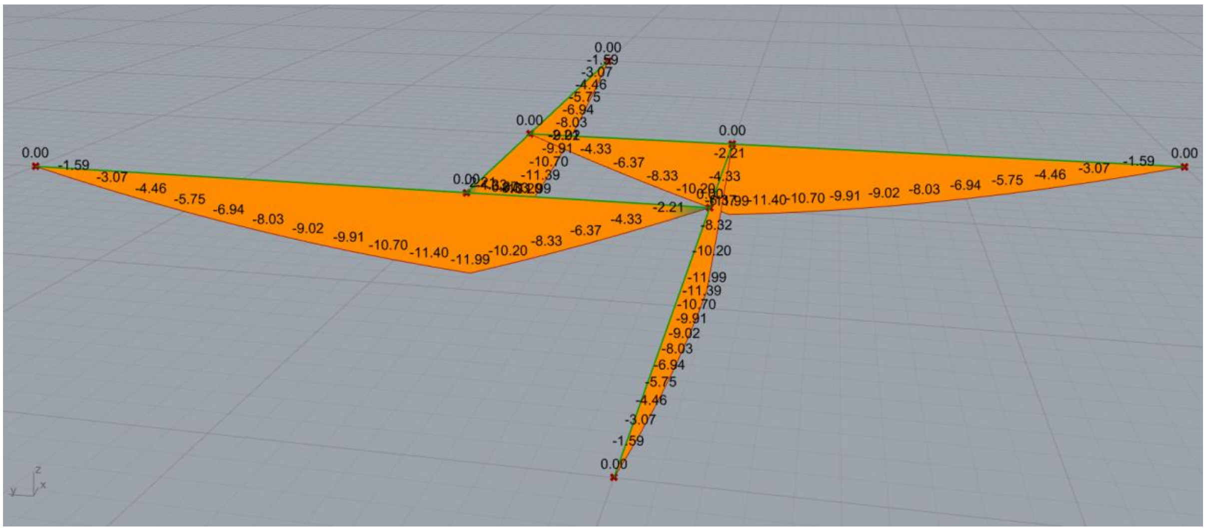

Figure A.1.1.: Moment distribution of RF-unit with hinged connections

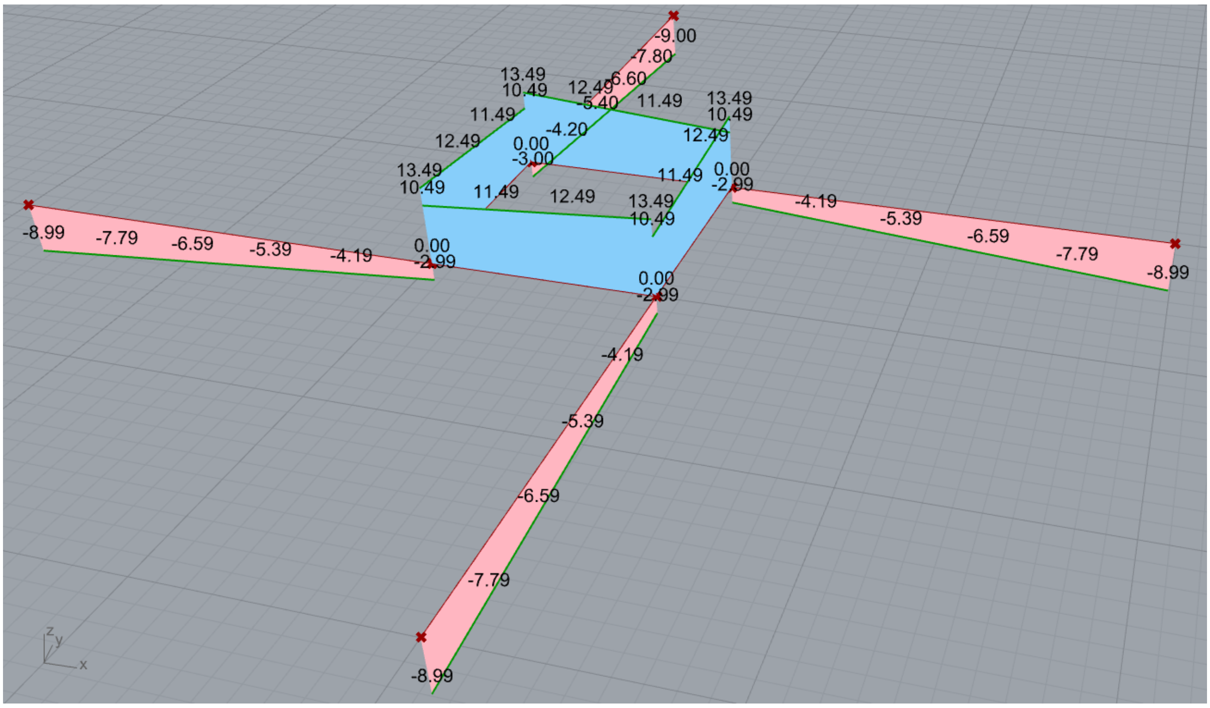

Figure A.1.2.: Shear force distribution of RF-unit with hinged connections

A.2. RF-unit with fixed connections

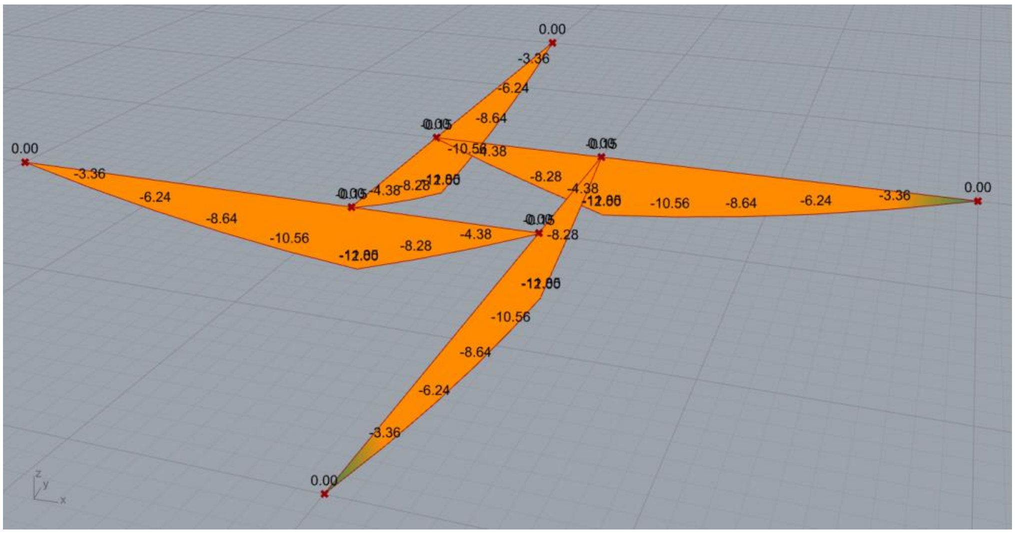

Figure A.2.1.: Bending moment distribution of RF-unit with fixed connections

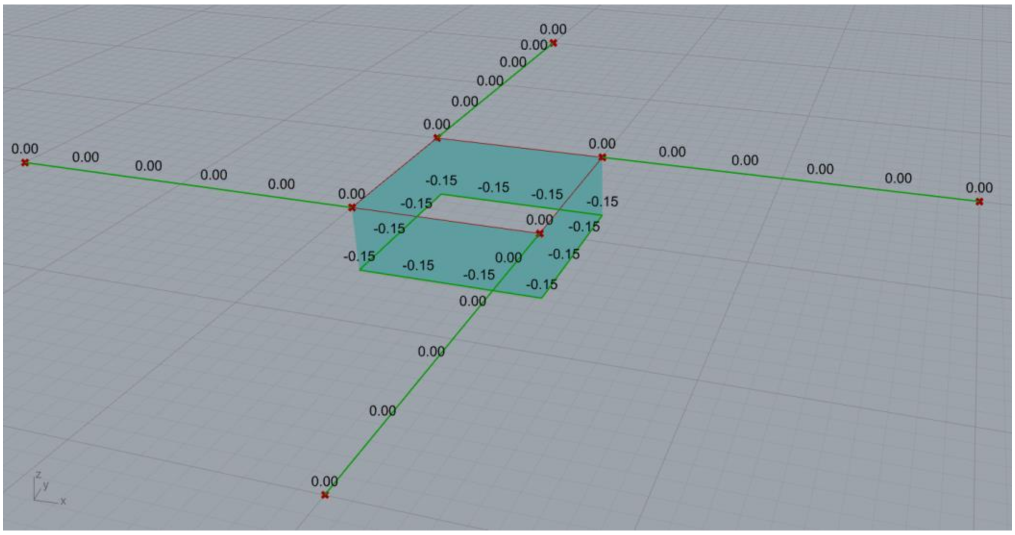

Figure A.2.2.: Torsional moment distribution of RF-unit with fixed connections

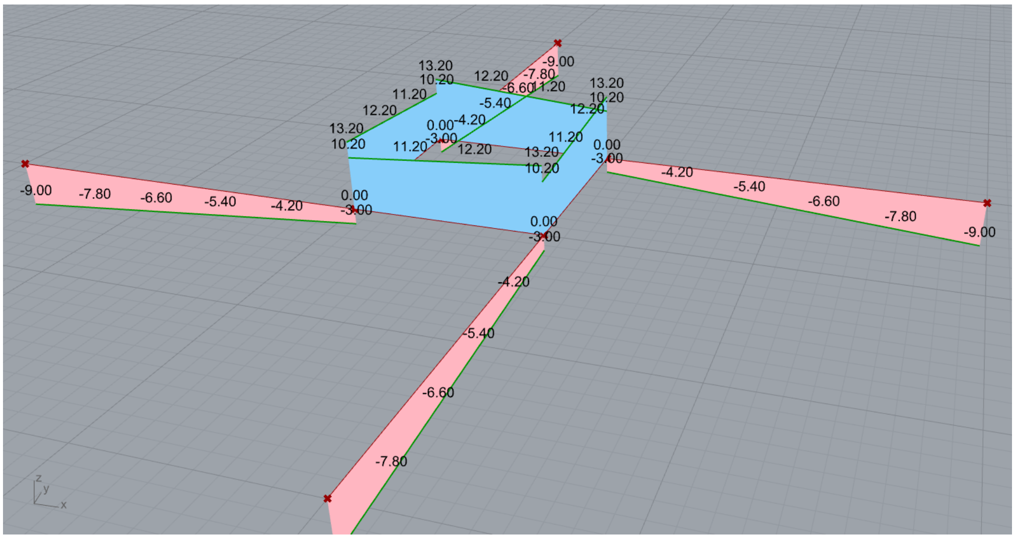

Figure A2.3.: Shear force distribution of RF-unit with fixed connections

B. One-way mirrored span: section forces distribution

B.1. Engagement length: 0.2 meter

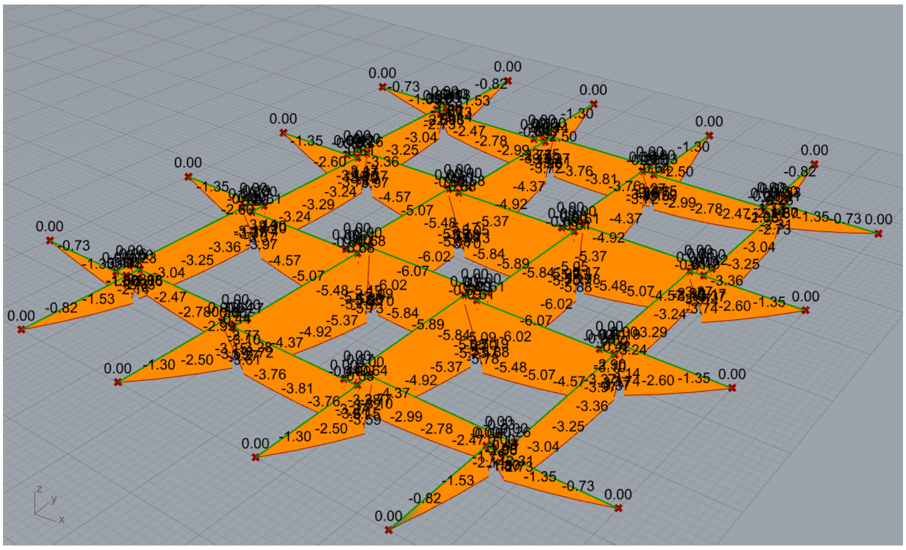

Figure B.1.1.: Bending moment distribution for a one-way mirrored RF-structure with engagement length of 0.2 m

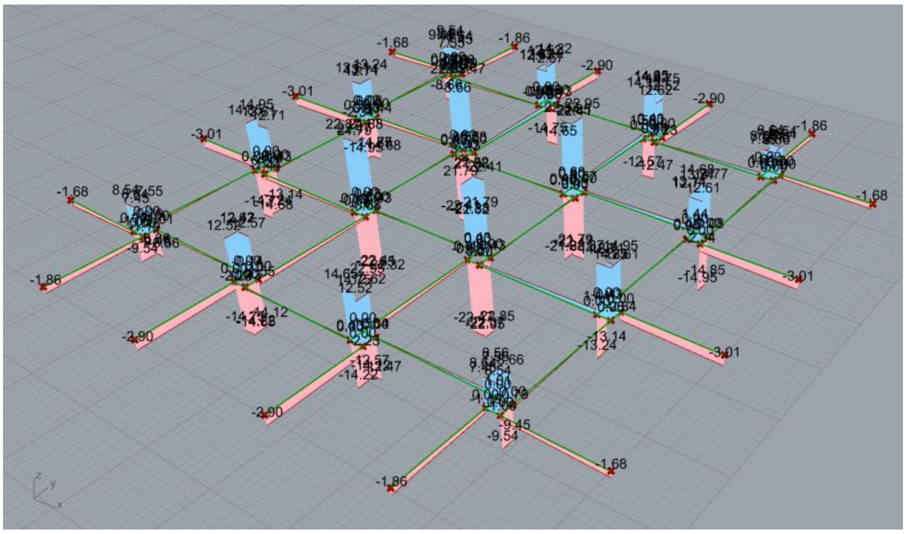

Figure B.1.2.: Shear force distribution for a one-way mirrored RF-structure with engagement length of 0.2 m

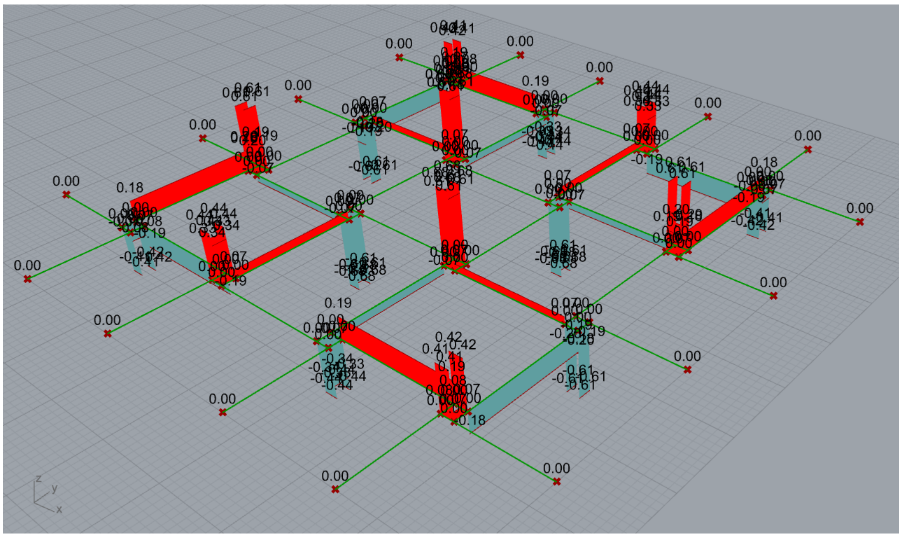

Figure B.1.3.: Torsional moment distribution for a one-way mirrored RF-structure with engagement length of 0.2 m

B.2. Engagement length: 0.4 meter

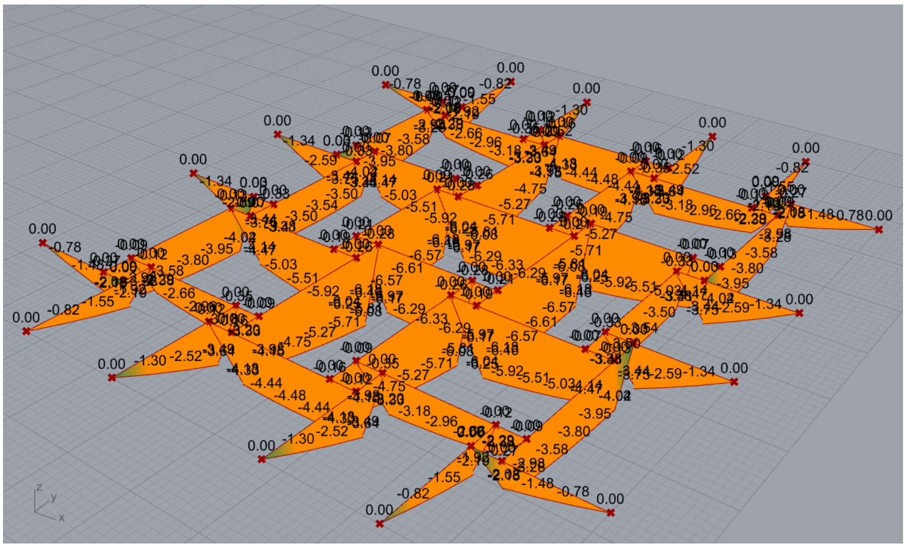

Figure B.2.1.: Bending moment distribution for a one-way mirrored RF-structure with engagement length of 0.4 m

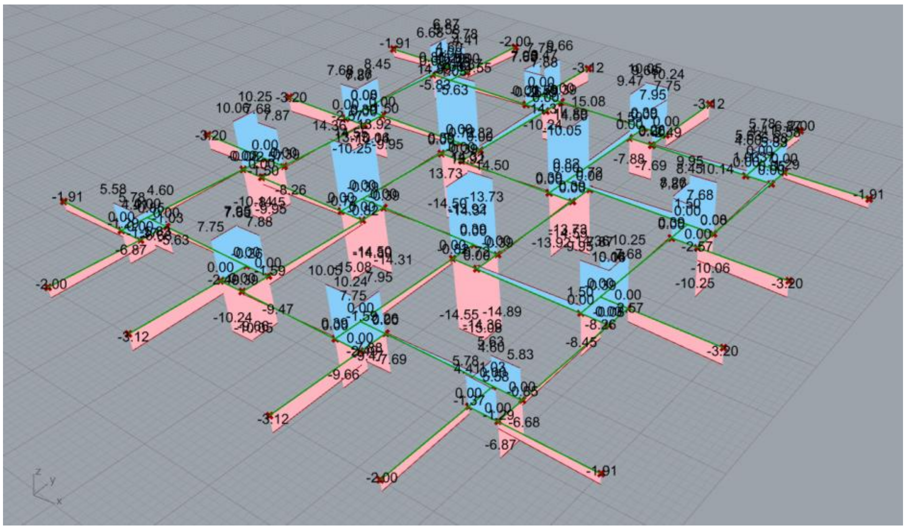

Figure B.2.2.: Shear force distribution for a one-way mirrored RF-structure with engagement length of 0.4 m

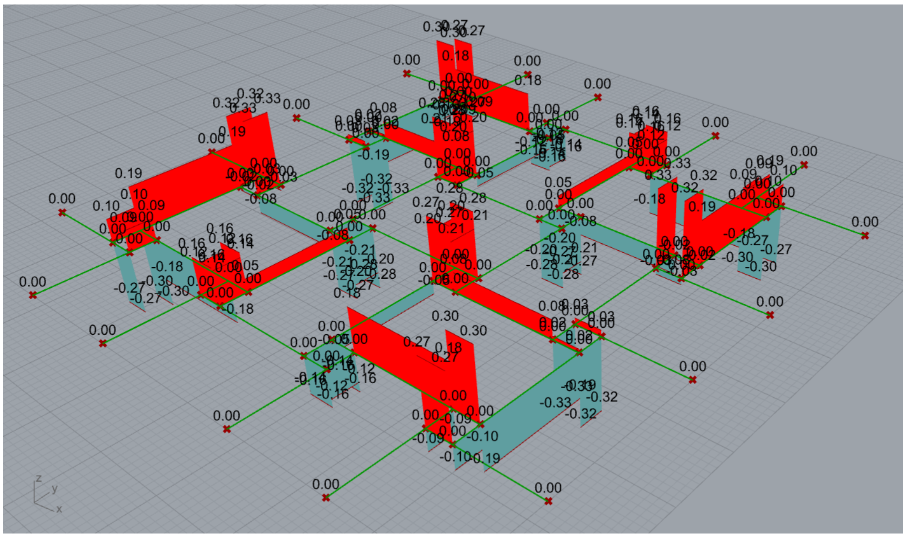

Figure B.2.3.: Torsional moment distribution for a one-way mirrored RF-structure with engagement length of 0.4 m

B.3. Engagement length: 0.6 meter

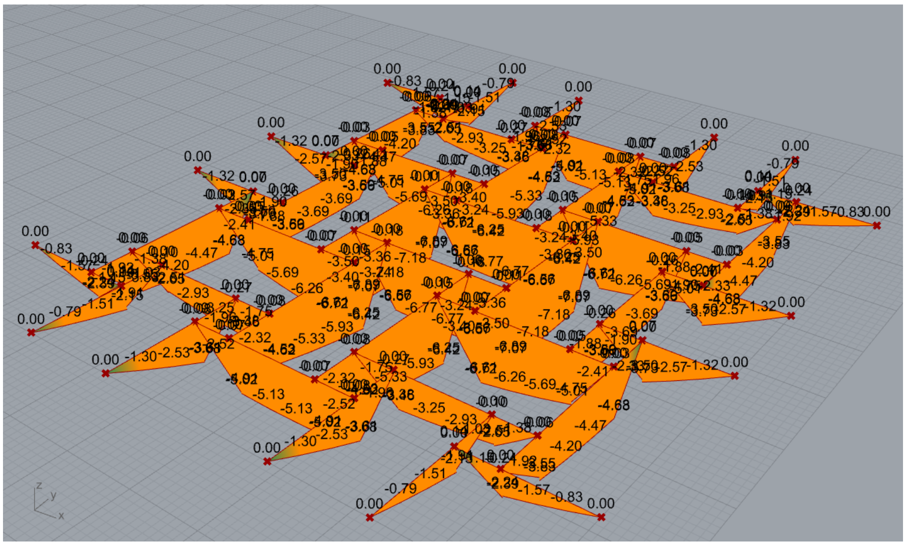

Figure B.3.1.: Bending moment distribution for a one-way mirrored RF-structure with engagement length of 0.6 m

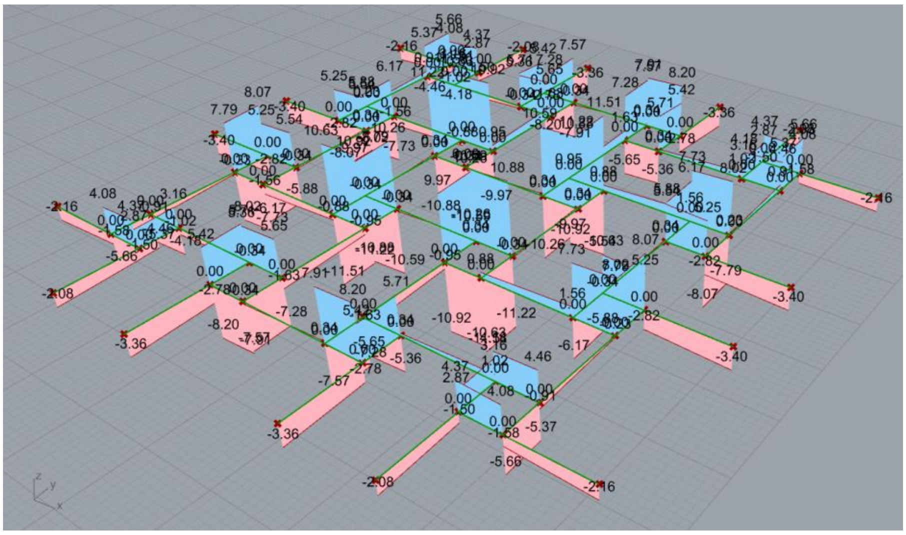

Figure B.3.2.: Shear force distribution for a one-way mirrored RF-structure with engagement length of 0.6 m

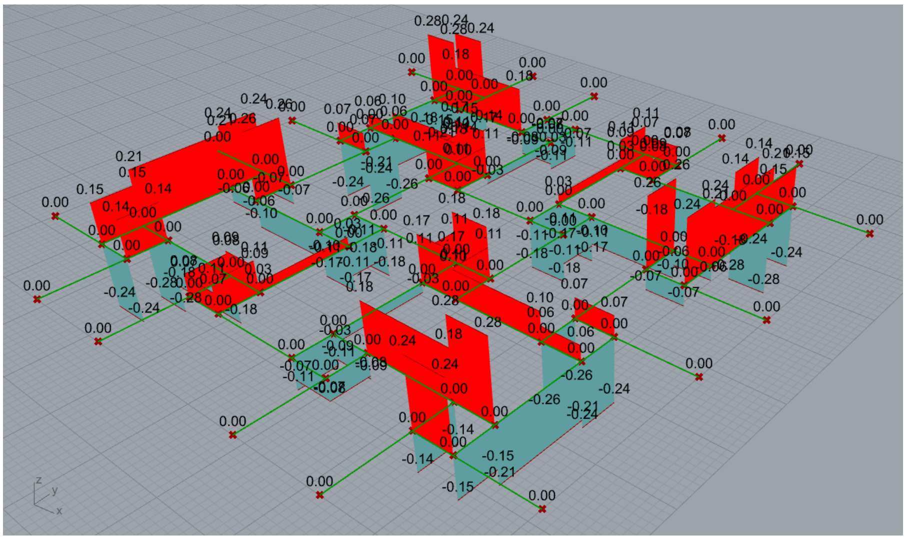

Figure B.3.3.: Torsional moment distribution for a one-way mirrored RF-structure with engagement length of 0.6 m

B.4. Engagement length: 0.8 meter

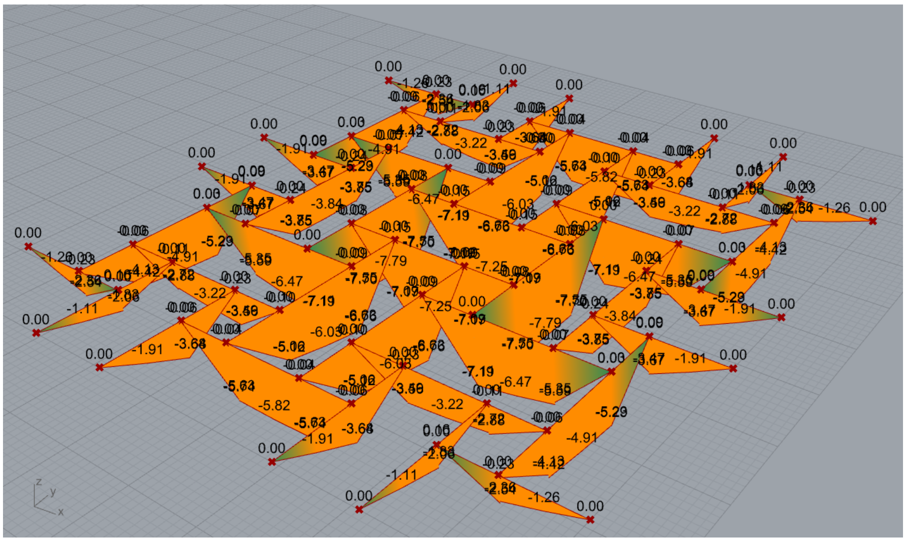

Figure B.4.1.: Bending moment distribution for a one-way mirrored RF-structure with engagement length of 0.8 m

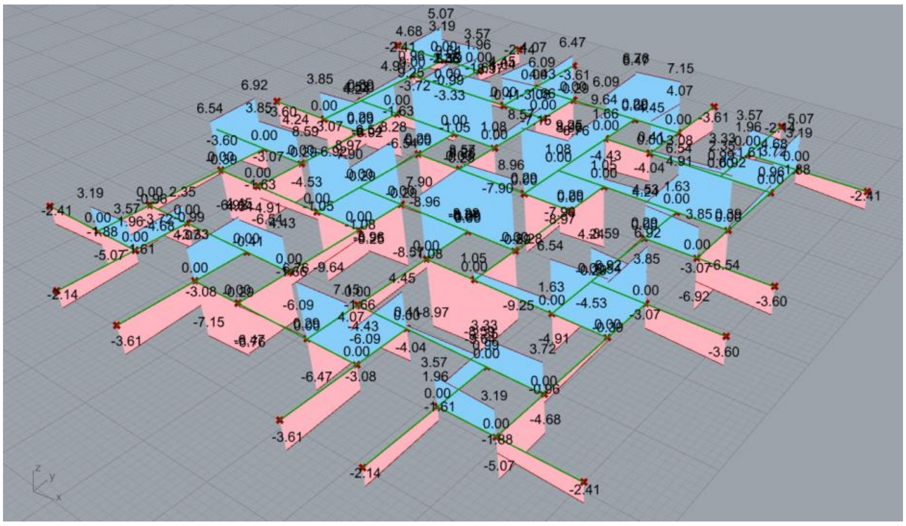

Figure B.4.2.: Shear force distribution for a one-way mirrored RF-structure with engagement length of 0.8 m

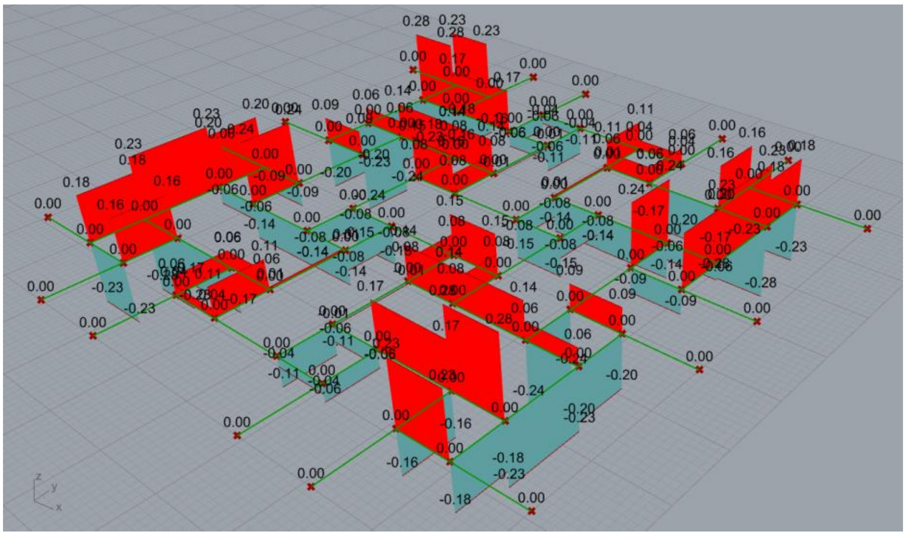

Figure B.4.3.: Torsional moment distribution for a one-way mirrored RF-structure with engagement length of 0.8 m

B.5. Engagement length: 1.0 meter

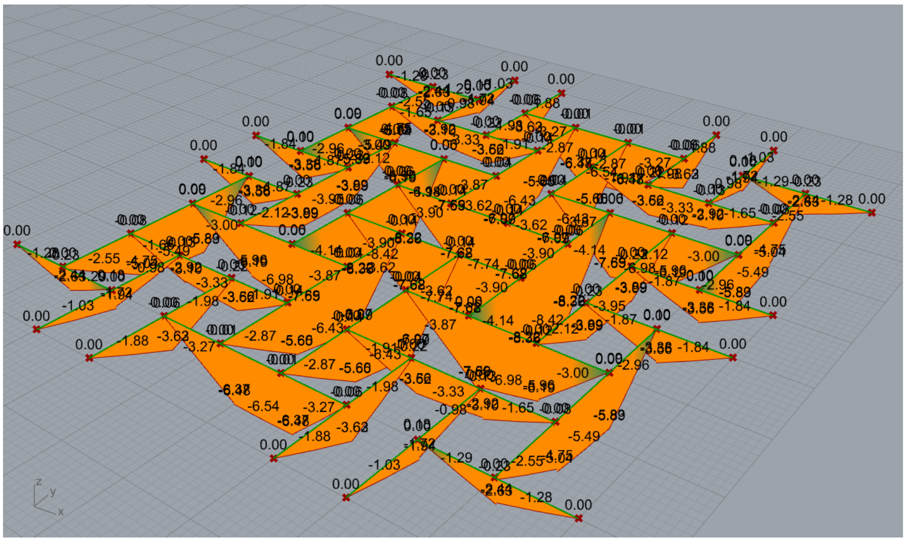

Figure B.5.1.: Bending moment distribution for a one-way mirrored RF-structure with engagement length of 1.0 m

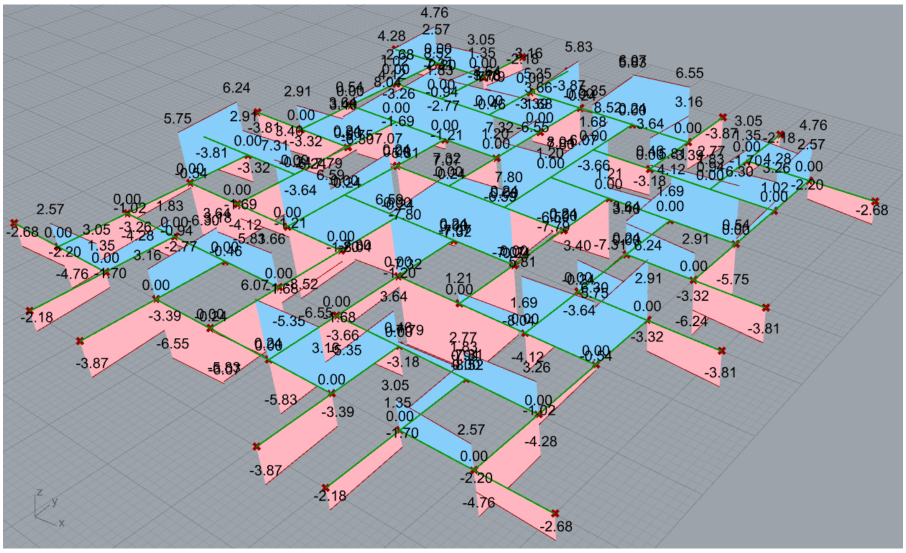

Figure B.5.2.: Shear force distribution for a one-way mirrored RF-structure with engagement length of 1.0 m

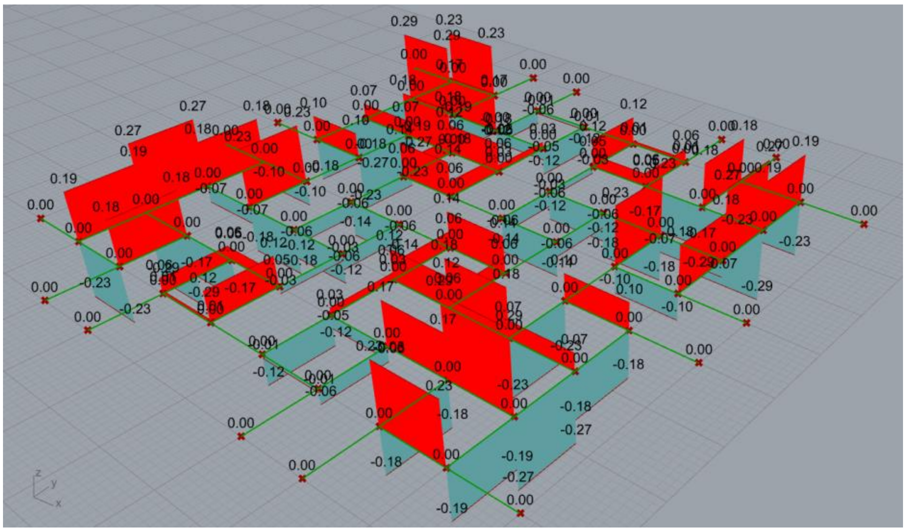

Figure B.5.3.: Torsional moment distribution for a one-way mirrored RF-structure with engagement length of 1.0 m

B.6. Engagement length: 1.2 meter

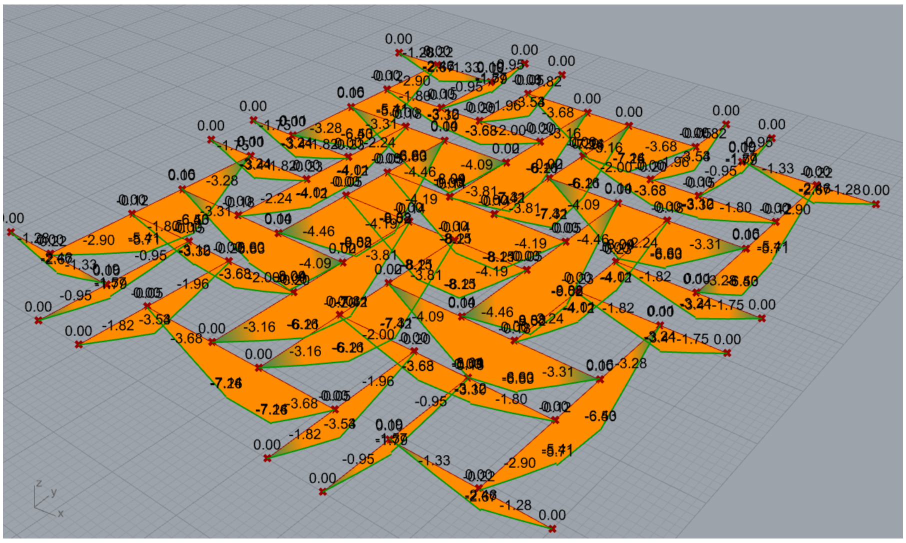

Figure B.6.1.: Bending moment distribution for a one-way mirrored RF-structure with engagement length of 1.2 m

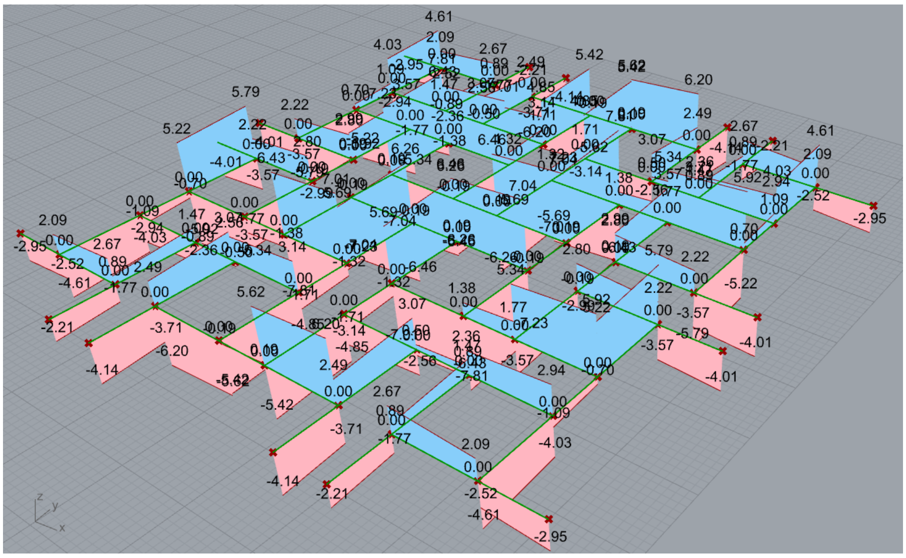

Figure B.6.2.: Shear force distribution for a one-way mirrored RF-structure with engagement length of 1.2 m

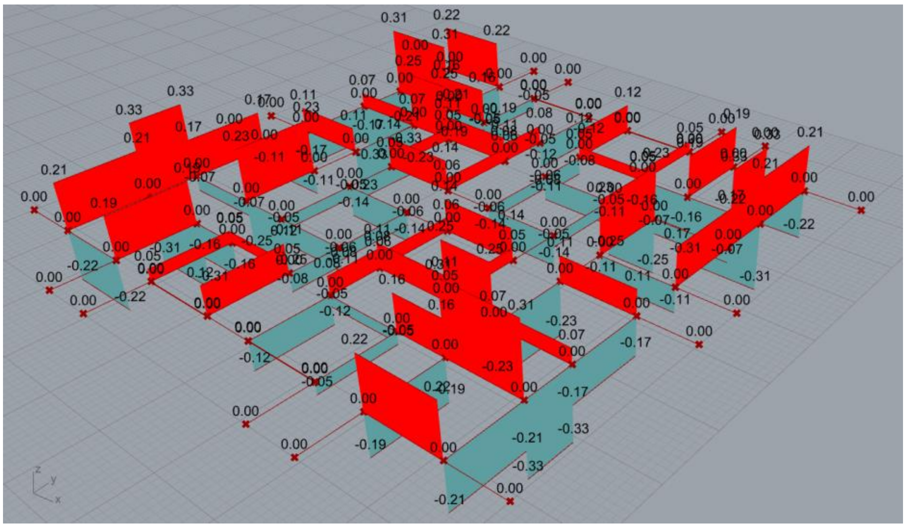

Figure B.6.3.: Torsional moment distribution for a one-way mirrored RF-structure with engagement length of 1.2 m

B.7. Engagement length: 1.4 meter

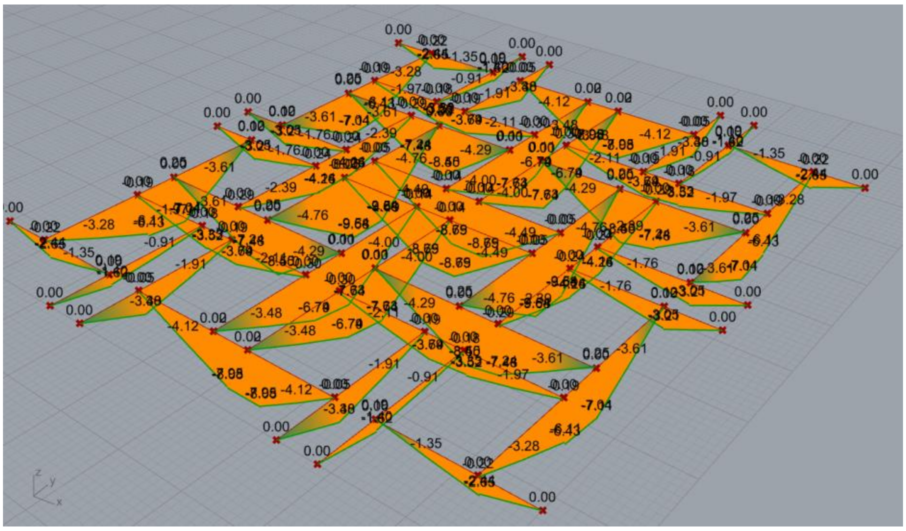

Figure B.7.1.: Bending moment distribution for a one-way mirrored RF-structure with engagement length of 1.4 m

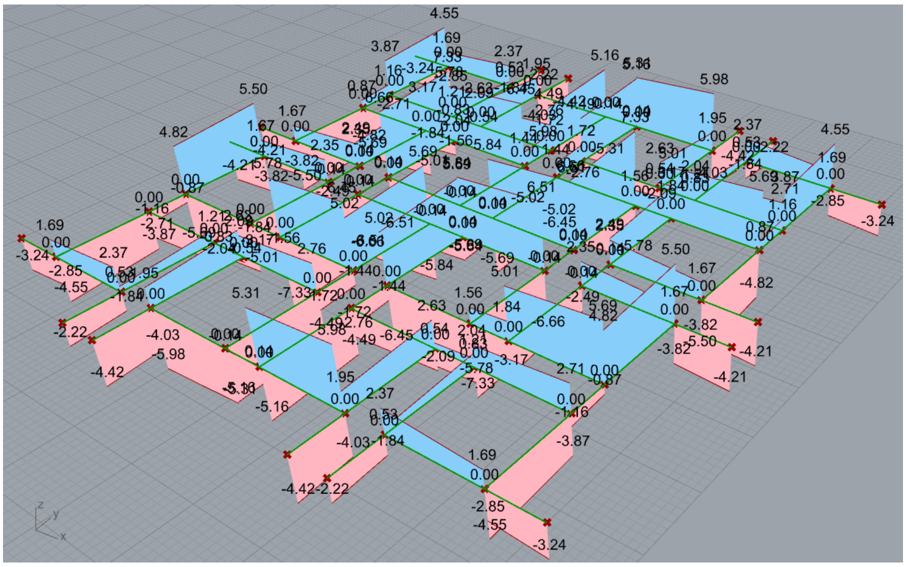

Figure B.7.2: Shear force distribution for a one-way mirrored RF-structure with engagement length of 1.4 m

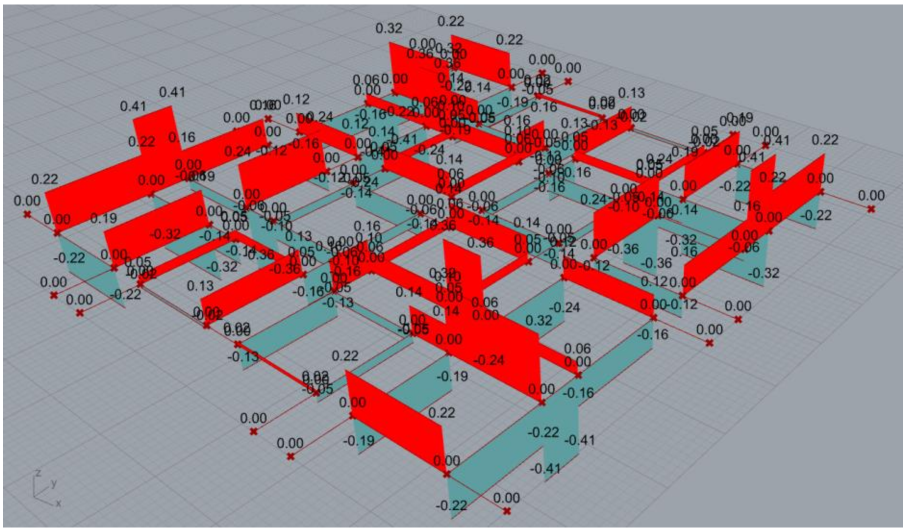

Figure B.7.3.: Torsional moment distribution for a one-way mirrored RF-structure with engagement length of 1.4 m

B.8. Engagement length: 1.6 meter

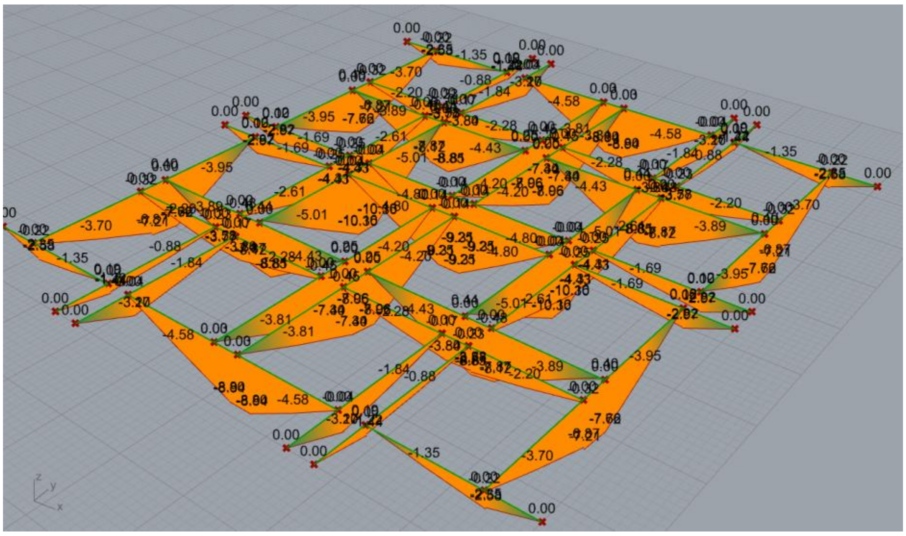

Figure B.8.1.: Bending moment distribution for a one-way mirrored RF-structure with engagement length of 1.6 m

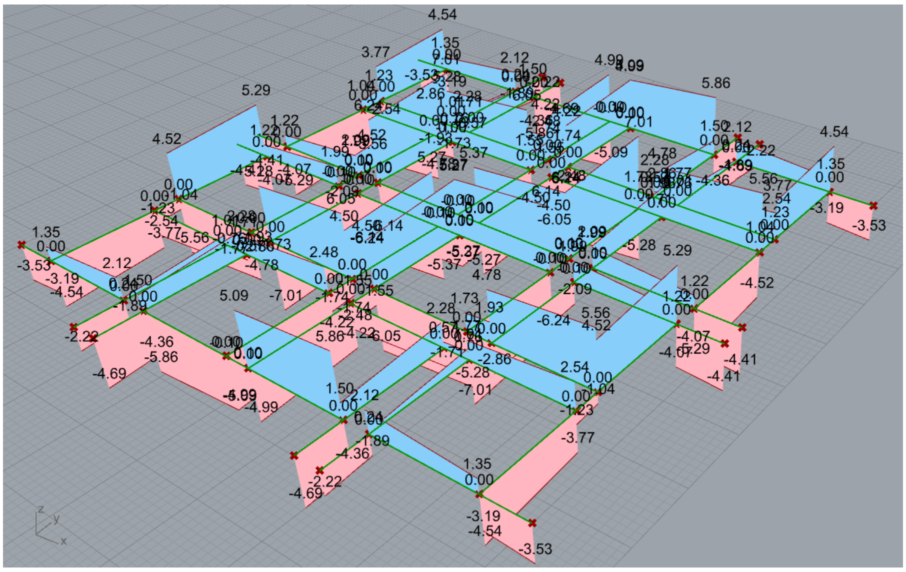

Figure B.8.2.: Shear force distribution for a one-way mirrored RF-structure with engagement length of 1.6 m

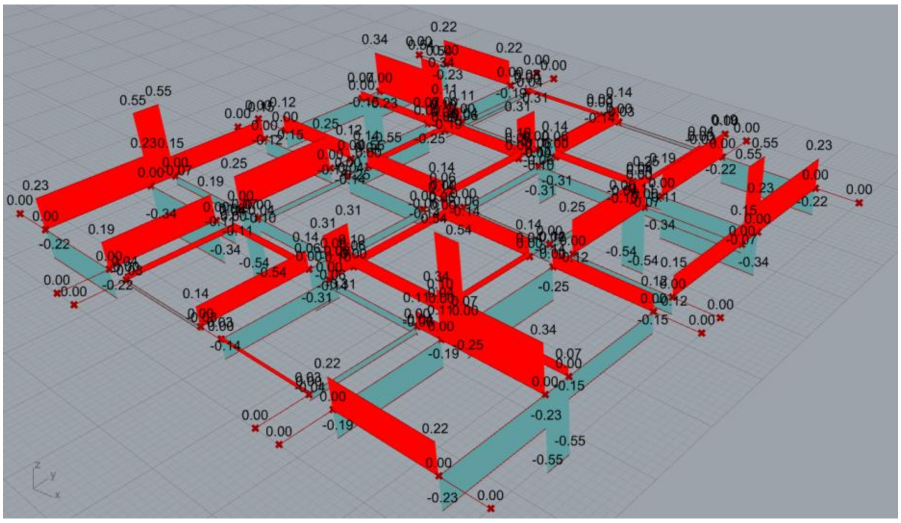

Figure B.8.3.: Torsional moment distribution for a one-way mirrored RF-structure with engagement length of 1.6 m

B.9. Engagement length: 1.8 meter

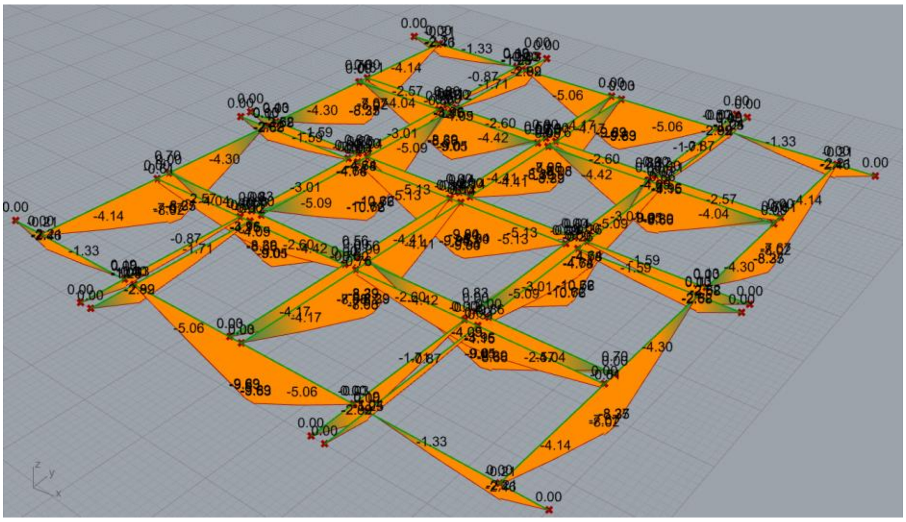

Figure B.9.1.: Bending moment distribution for a one-way mirrored RF-structure with engagement length of 1.8 m

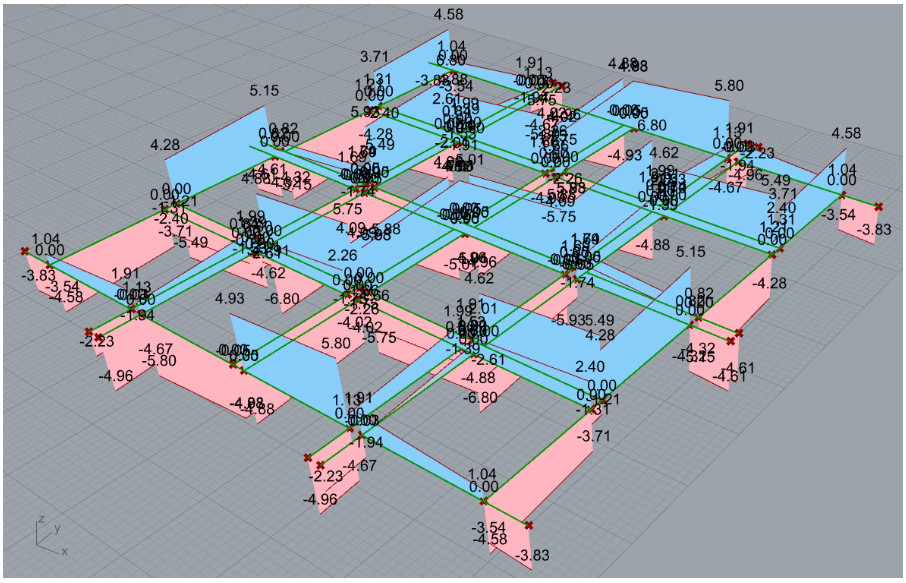

Figure B.9.2.: Shear force distribution for a one-way mirrored RF-structure with engagement length of 1.8 m

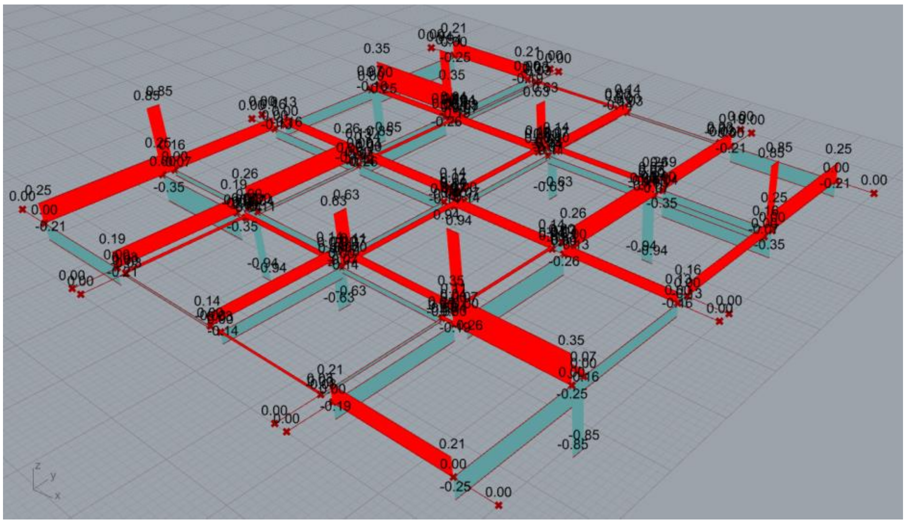

Figure B.9.3.: Torsional moment distribution for a one-way mirrored RF-structure with engagement length of 1.8 m

C. Two-way mirrored span: section forces distribution

C.1. Engagement length: 0.2 meter

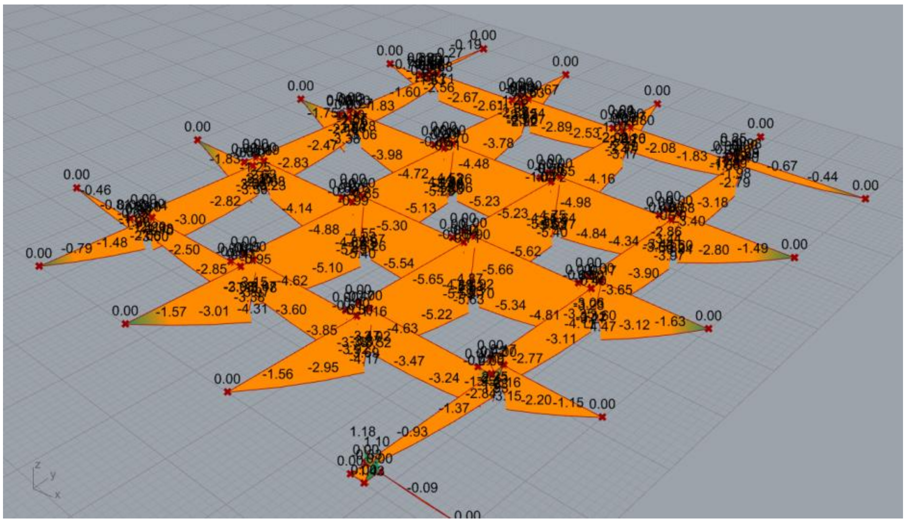

Figure C.1.1.: Bending moment distribution for a two-way mirrored RF-structure with engagement length of 0.2 m

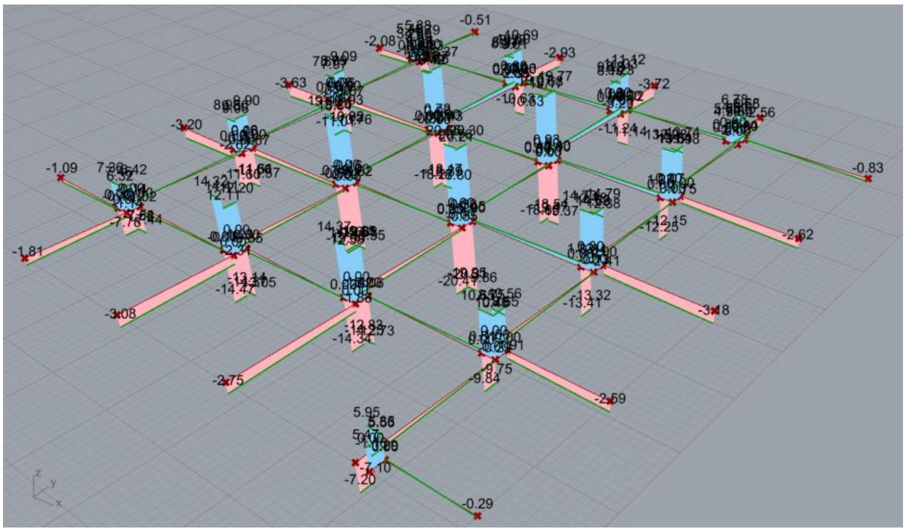

Figure C.1.2.: Shear force distribution for a two-way mirrored RF-structure with engagement length of 0.2 m

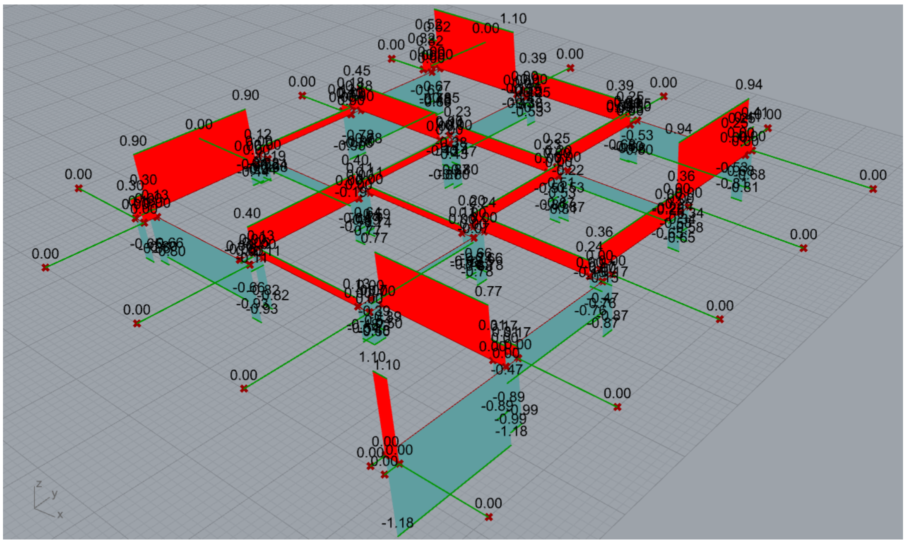

Figure C.1.3.: Torsional moment distribution for a two-way mirrored RF-structure with engagement length of 0.2 m

C.2. Engagement length: 0.6 meter

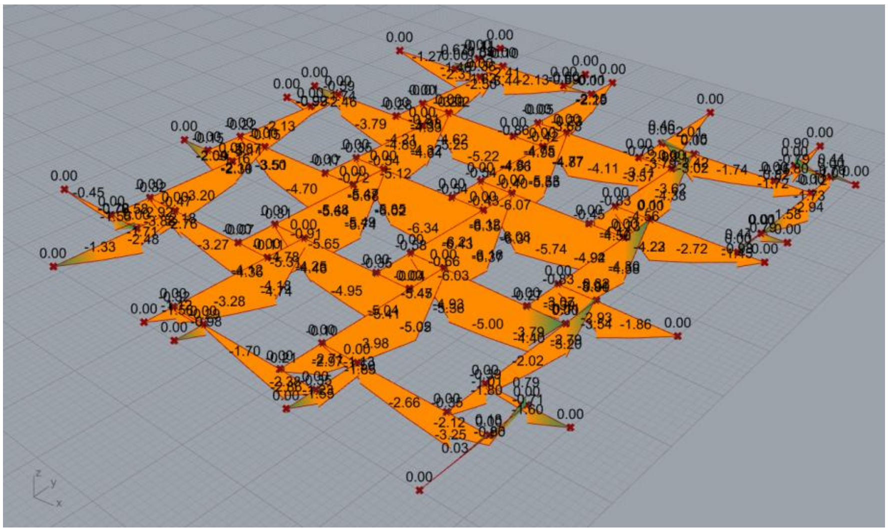

Figure C.2.1.: Bending moment distribution for a two-way mirrored RF-structure with engagement length of 0.6 m

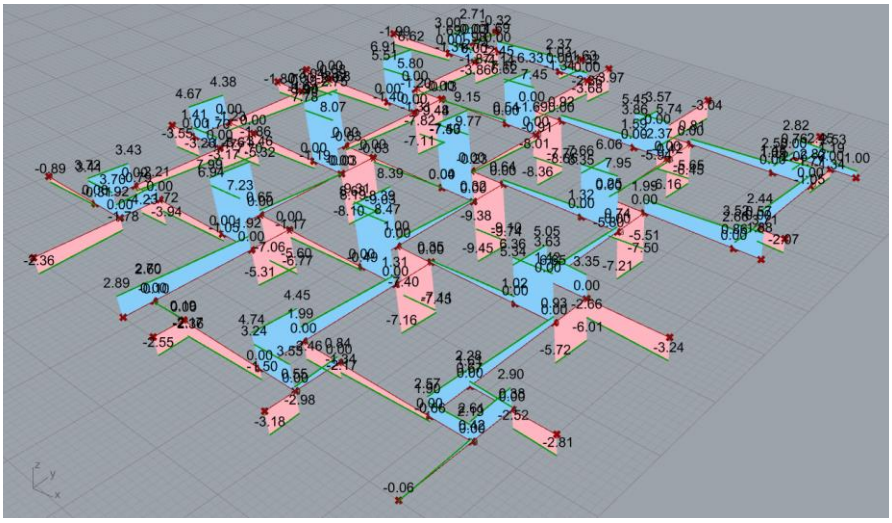

Figure C.2.2.: Shear force distribution for a two-way mirrored RF-structure with engagement length of 0.6 m

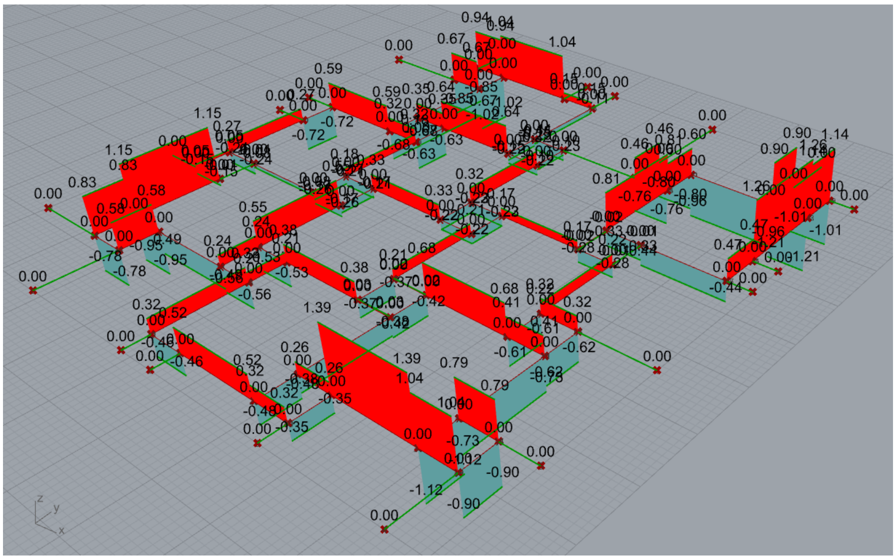

Figure C.2.3.: Torsional moment distribution for a two-way mirrored RF-structure with engagement length of 0.6 m

C.3. Engagement length: 1.0 meter

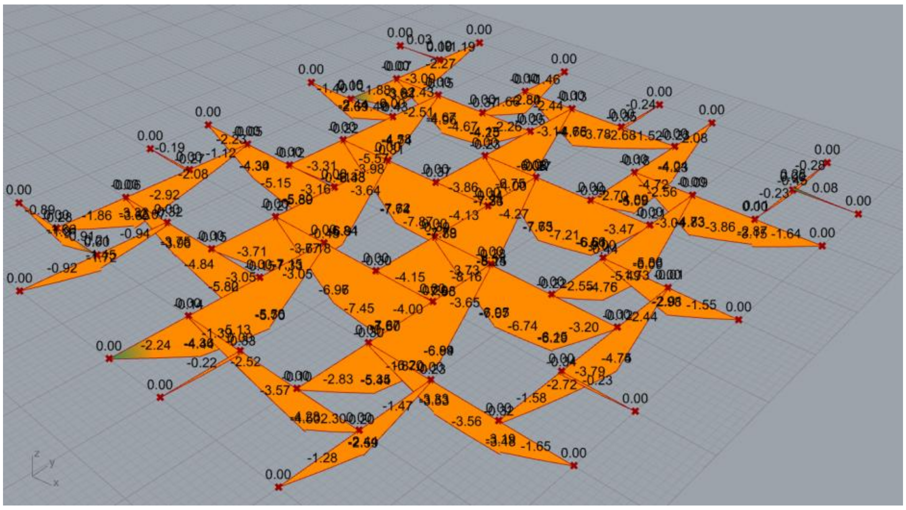

Figure C.3.1.: Bending moment distribution for a two-way mirrored RF-structure with engagement length of 1.0 m

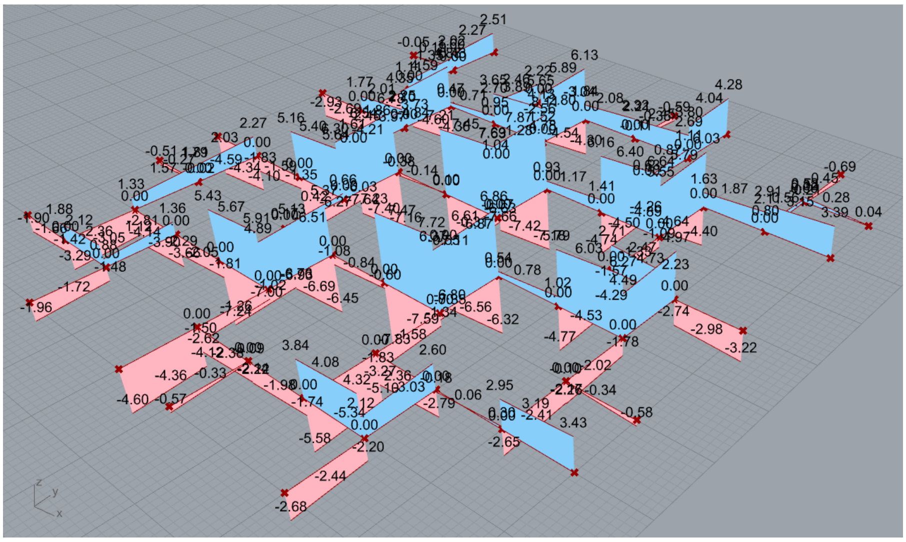

Figure C.3.2.: Shear force distribution for a two-way mirrored RF-structure with engagement length of 1.0 m

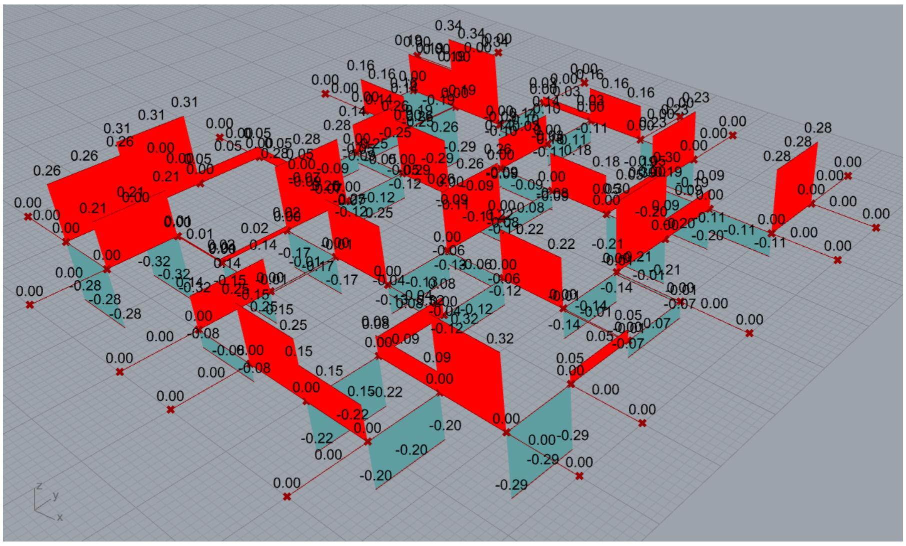

Figure C.3.3.: Torsional moment distribution for a two-way mirrored RF-structure with engagement length of 1.0 m

C.4. Engagement length: 1.4 meter

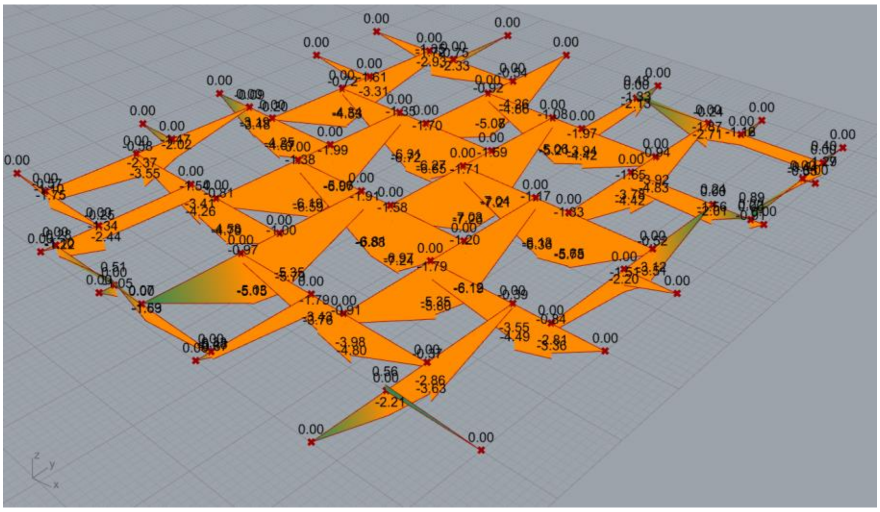

Figure C.4.1.: Bending moment distribution for a two-way mirrored RF-structure with engagement length of 1.4 m

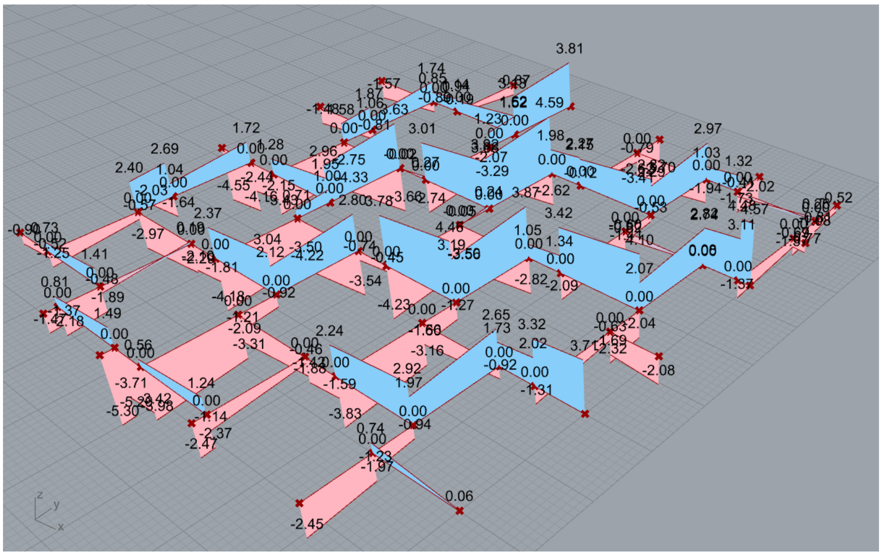

Figure C.4.2.: Shear force distribution for a two-way mirrored RF-structure with engagement length of 1.4 m

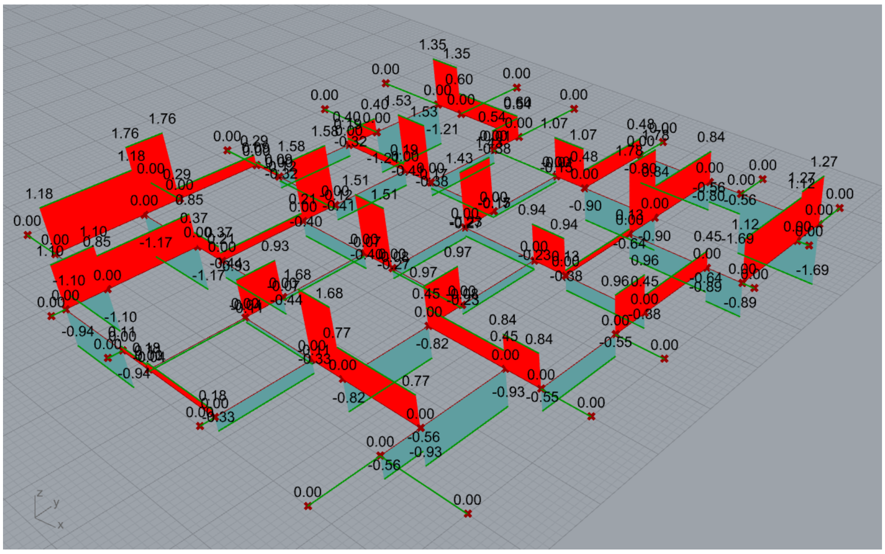

Figure C.4.3.: Torsional moment distribution for a two-way mirrored RF-structure with engagement length of 1.4 m

C.5. Engagement length: 1.8 meter

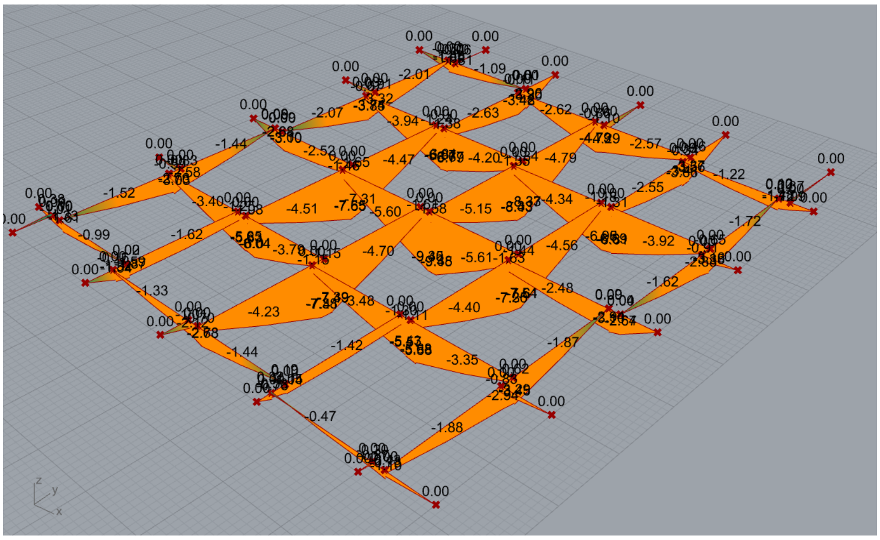

Figure C.5.1.: Bending moment distribution for a two-way mirrored RF-structure with engagement length of 1.8 m

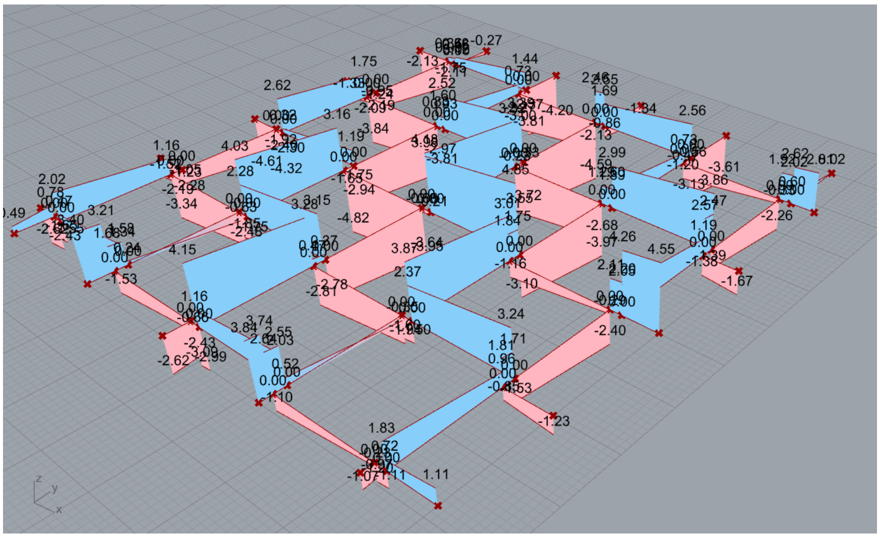

Figure C.5.2.: Shear force distribution for a two-way mirrored RF-structure with engagement length of 1.8 m

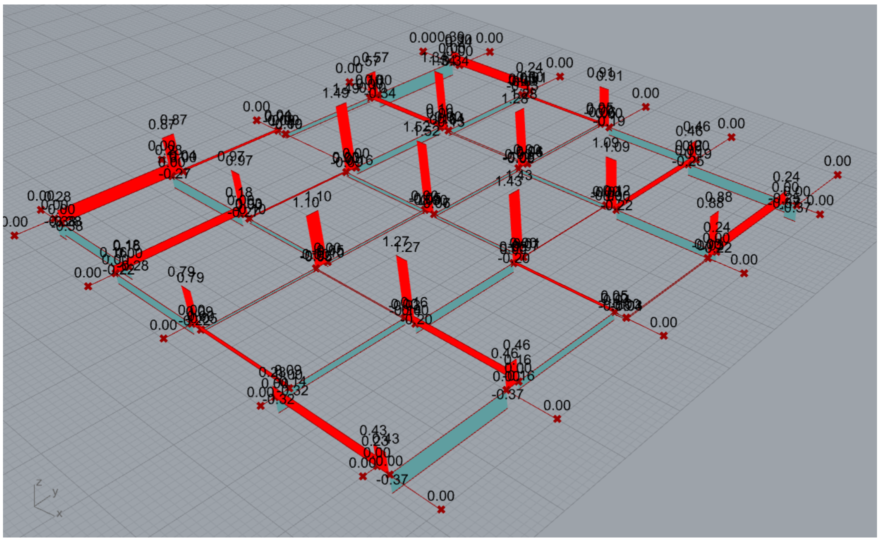

Figure C.5.3.: Torsional moment distribution for a two-way mirrored RF-structure with engagement length of 1.8 m